university of groningen / faculty of science and engineering

Activity and regenerability study of supported Ru catalysts for Kraft lignin hydrotreatment

MsC thesis

F.E. Heins

16-7-2017

1st supervisor: Prof. Dr. Ir. H.J. Heeres
2nd supervisor: Dr. P.J. Deuss
Daily supervisor: Dr. I. Hita

Table of content

Abstract

The potential of lignin as feedstock for biobased chemicals in biorefinery schemes has attracted high research interest in the recent years. Particularly, Kraft lignin (the most commercially available type of lignin) provides an optimal aromatic based structure for the production of biochemicals (i.e. alkylphenolics, aromatics). However, the high sulfur content in Kraft lignin and the harsh conditions during hydrotreatment imply a major challenge due to catalyst deactivation.

In this research, we present the results for the catalytic hydrotreatment of Kraft lignin using Ru-based catalysts on various supports (Al_2O_3, SiO_2, ZrO_2 and TiO_2) with different metal loadings (0.3 and 1 wt%). Catalyst deactivation was explored by performing a second reaction cycle using regenerated catalysts, the results were correlated with BET analysis, XRD and TEM analysis. The reactions were performed in a batch autoclave at 450°C, 100 bars of initial hydrogen pressure and 4 h of reaction time. Lignin oil yields between 35-40 wt% and monomeric products yields between 28-31 wt% on lignin intake have been obtained. The 1%Ru-TiO_2 catalyst showed the most promising results with a lignin oil yield of 39.6 wt% and high yields of alkylphenolics (16.1 wt%) and aromatics (4.5 wt%) on lignin intake and interestingly, the 0.3%Ru-TiO_2 catalysts showed similar results.

During the hydrotreatment 17-22 wt% of coke was formed, based on the lignin intake. Therefore, the catalysts were regenerated by coke combustion in air for 4h at 550°C, and tested for a second reaction cycle. The 1%Ru-TiO_2 catalyst was the only catalysts that showed similar reaction results after regeneration. The other regenerated catalysts showed a significant decrease in lignin oil yield (26-31 wt%) and monomeric products yield (19-25 wt%). Out of all the regenerated catalysts, the 1%Ru-TiO_2 catalyst was the only catalysts that did not show a significant increased size and clustering of Ru particles, which correlates to the similar performance in fresh and regenerated conditions. The regenerability of the 1%Ru-TiO_2 catalyst was further explored in a recycling study. During the 3 cycles, the lignin oil and monomeric products yields steadily decreased. Showing that the catalyst gradually loses activity after regeneration.

Despite the presence of sulfur, the Ru-based catalysts showed high oil and monomeric products yields when the results were compared with previous studies. In fresh conditions, the catalysts did not show significant differences in reaction products yields when various supports and metal loadings were used. Major differences in reaction products yields were observed when regenerated catalysts were applied, this was mainly ascribed to the instability of catalytic support, increasing size and clustering of Ru particles.

1. Introduction

The depletion of fossil resources used for fuels, chemicals and energy has boosted research in renewable resources. Renewable electric energy sources are already commercialized, such as wind-, solar-, tidal- and geothermal energy. However, for the requirement of carbon-based alternatives such as: transportation fuels, materials and chemicals biomass is considered an interesting feedstock. Biomass is already used for fuel and energy purposes (e.g. bioethanol, biodiesel, and biogas). (1) The use of first generation biomass has caused concerns since this type of biomass is also suitable for food production. Examples of first generation biomass products are bioethanol from sugar/starch and biodiesel from vegetable oils. Current focus is on obtaining fuels, energy and chemicals from lignocellulosic biomass, also referred to as second generation biomass. (2) The development of bioethanol as a fuel and biobased chemicals, such as lactic acid, succinic acid and levullinic acid, are examples of value-added products obtained from second generation biomass. (1)

Lignin

In non-edible lignocellulosic biomass, cellulose, hemicellulose and lignin are the three main components. Lignin is an amorphous, polyphenolic thermoset with a highly complex three-dimensional structure and is the third largest biopolymer in lignocellulosic biomass. The rigidity of lignin gives the plants tissue strength and hydrophobicity. (1) The three most important building blocks of lignin are coumaryl alcohol, coniferyl alcohol, and syringyl alcohol which can be seen in Fig 1.1 (3). Different types of linkages are formed between the aromatic monomers, the most common linkages are the β-0-4, α-0-4, β-5 and 5-5. During lignin depolymerization, these linkages are cleaved, leading to a variety of aromatic and platform chemicals. This makes lignin an interesting starting material for the production of biochemicals. (1) However, unfavorable reactions are observed during lignin depolymerization including recondenzation and overreduction of aromatic rings, which ultimately leads to coke formation. Also, the complex and amorphous structure of lignin makes it challenging to produce specific molecules during depolymerization. (4)

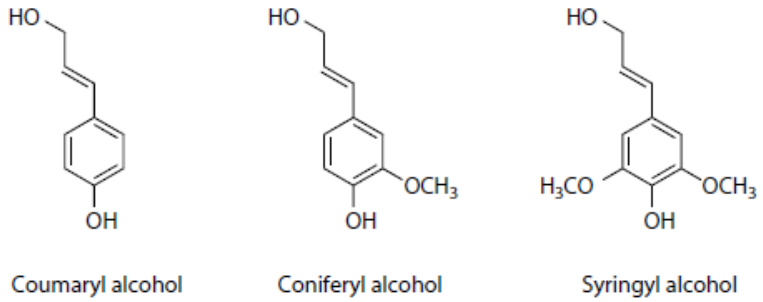

Fig. 1.1 Three main building blocks of lignin (3)

During wood pulping (Kraft process), lignin and hemicellulose (black liquor) are separated from the cellulose fibers which are further treated to produce wood pulp and can eventually be used for paper production. The black liquor is considered a side product of the process. Multiple pulping techniques are applied for this treatment such as orgnasolv, soda and Kraft pulping. The organosolv pulping process is a collective term for pulping performed in organic solvents and is considered more environmental-friendly then conventional pulping processes. (5) However, organosolv processes are costly due to expensive chemicals and equipment (6). The soda pulping process uses sodium carbonate as a solvent and is the predecessor of the Kraft pulping process. In the Kraft pulping process, the sodium carbonate was replaced by sodium sulfate and became the dominant wood pulping process because of the recyclability of the chemicals. The dominance of the Kraft pulping process and the abundance of Kraft lignin make it an interesting feedstock for the production of bio-based platform chemicals. (5) (7)

Kraft pulping

In the Kraft pulping process, lignin is considered a side product and is mainly used as a low-energy fuel to generate heat, used in the process. Preferable, the aromatic rich structure of Kraft lignin is used for the production of valuable chemicals to increase the economic value of Kraft lignin (8). Also, the abundance of Kraft lignin makes it a favorable feedstock for biochemicals. Annually, 40-50Mt of Kraft lignin is produced (9). The harsh conditions during the Kraft process change the chemical structure of the native lignin due to a variety of reactions: cleavage of the β-0-4 and β-ether linkages, C-C crosslinking and condensation reactions. (5) Furthermore, the application of sodium sulfide in the Kraft lignin process introduces thiol groups on the lignin structure. This can be seen in the model structure for Kraft pine lignin in Fig 1.2 (10). The sulfur content of Kraft lignin is 2-3% (9).

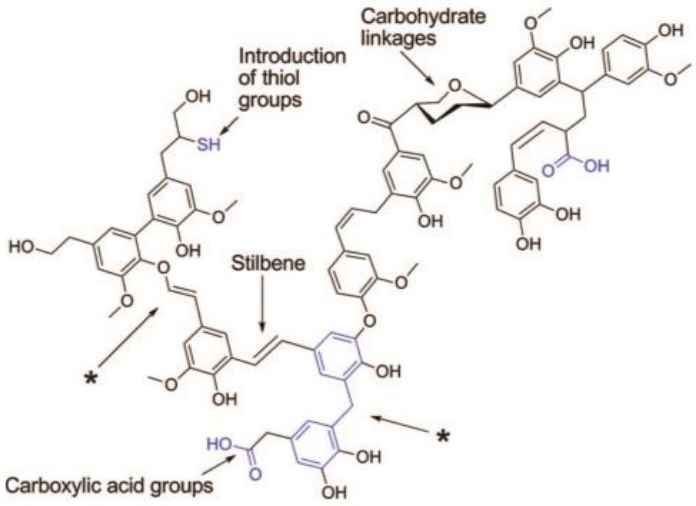

Fig. 1.2 Model structure for Kraft pine lignin (10)

Multiple technologies are reported regarding the depolymerization of lignin. These include depolymerization by enzymes (11), base catalysis (12), catalytic hydrotreatment (1) (9) and oxidative depolymerization (13). A comparison between oxidative and reductive treatment shows that different products are obtained. The reductive cleavage of C-C and C-H bonds results in a variety of monomeric compounds, for example phenols, benzene, toluene and xylene. The oxidative cleavage of C-C and C-H bonds results in vanillin and similar compounds. Simultaneously, undesired free radical formation and condensation reactions occur during oxidative treatment. Therefore, reductive treatment is considered more favorable (14).

Biobased chemicals

Lignin provides an optimal aromatic-based structure for the production of biochemicals. In Fig 1.3, some of the many compounds derived from lignin are depicted. The production of alkylphenolics from lignin finds a great economic potential due to their many application, such as: additives to plastics, agricultural chemicals and non-ionic surfactants (used for detergents, dispersants and solubilizers) (15). Also, aromatics derived from lignin find many applications in industry, such as: industrial solvents (benzene and toluene), polymer synthesis (styrene), fuel additives and starting material for many chemical synthesis (16). A condensation reaction between lignin-derived alkylphenolics results in Bishenol-A (BPA) which is used for the synthesis of polycarbonates and epoxy resins and is produced in large volumes (5.4 Mt in 2015). However, the leaching of BPA has caused major health concerns due to interference with hormones which has boosted research in alternative compounds. A promising alternative for BPA is Bisguaiacol F which can be produced from lignin-derived guaicols. (17) (18) Lignin-derived cyclohexanols can be applied as precursors for polymer building blocks such as: caprolactam, caprolactone and adipic acid. Also, alkylsubstituted cyclohexans are derived from

lignin and can be used for polymer synthesis of alkylated variants which give opportunities for tuning the polymers physical properties. (19) Previous studies by Kumar et al. (9) have proven that catalytic Kraft lignin hydrotreatment yields the aforementioned chemicals since mainly alkylphenolics and aromatics, but also cyclic alkanes, linear/branched alkanes, polycyclic aromatics, ketones, alcohols, acids, guaiacols, and catechols were observed in the lignin oil.

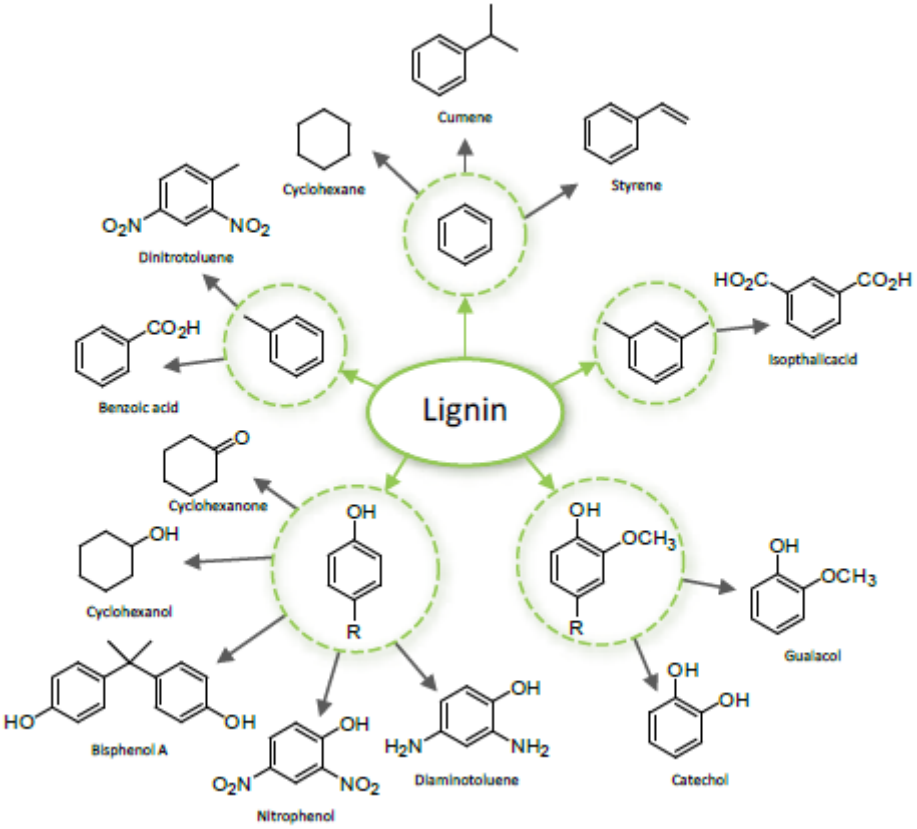

Fig. 1.3 Overview of lignin-derived compounds (1)

Catalytic hydrotreatment

During catalytic hydrotreatment, lignin reacts with hydrogen in the presence of a catalyst. Generally, the reaction temperature is within 200-450°C and hydrogen pressure is within 50- 250 bars. Catalysts are essential for lignin hydrotreatment due to the strength of the C-C and C-O bonds (14). Catalytic hydrotreatment of lignin results in depolymerization and hydrodeoxygenation, decreasing the oxygen content of the obtained lignin oil significantly in comparison with the original lignin. (1)

During the Kraft process, the more reactive bonds in lignin are cleaved. However, harsh process conditions are required to cleave the stronger bonds in lignin that will yield valuable monomers. The random structure and depolymerization of lignin yields a complex mixture of chemical compounds in the lignin oil. In a large-scale process, the lignin oil needs to be refined to yield monomers such as: alkylphenolics, aromatics, cyclohexanols and guaiacols, which can be used for a variety of application which were previously mentioned. (5)

Generally, the catalytic hydrotreatment of lignin is carried out in a solvent because it reduces char formation. Different types of lignin require different types of solvents because the dissolution of lignin is influenced by the structure, bonding properties and functional group density (5). Yuan et al. (20) recently explored the depolymerization of Kraft lignin in supercritical acetone. Supported Ni and Ru catalysts were applied under 100 bars initial hydrogen pressure at 300 and 350°C and 1 h of reaction time. Ru catalysts were more effective for

the depolymerization of Kraft lignin. Carbon-supported Ru (5 wt%) reduced the M_w of Kraft lignin from 10200 g mol^{-1} to 5300 g mol^{-1} and 1020 g mol^{-1} with reaction temperatures of respectively 300 and 350°C. De Wild et al. (21) used the same catalyst (Ru/C) for the hydrotreatment of pyrolytic lignin oil. Dodecane was used as a solvent under the conditions of 350°C, 100 bars of hydrogen and 2 h reaction time. After hydrotreatment, all the aromatic compounds in the pyrolytic lignin oil were converted into cycloalkanes, alkyl-substituted cyclohexanols, cyclohexanol and linear alkanes. Zhai et al. (22) used non-noble metals for the depolymerization of organosolv lignin in methanol. A Ni-Fe on activated carbon was used under the conditions of 225 °C, 20 bars of hydrogen, and 6 h reaction time. The total monomer yield after the reaction was 20.3 wt% with propylguaiacol and propylsyringol as main products.

In a large-scale process, use of a solvent would require an extensive recovery system. Furthermore, solvents are not always inert and may incorporate into the reaction products. For instance, as reported by Ma et al. (23) lignin depolymerization with a Mo catalyst (280°C) gave an oil yield of 160 wt% due to a large amount of ethanol condensation products. Therefore, a solvent-free approach would be preferred, based on the principle that Kraft lignin melts at circa 200°C and can act as its own solvent (9).

The solvent-free approach was recently explored by Kumar et al. with supported sulfided NiMo and CoMo catalysts (9), under 100 bars of initial hydrogen pressure at 350°C and 4 h of reaction time. The highest yield of alkylphenolics and aromatics was achieved with NiMo/MgO-La_2O_3 which gave 15.7 wt% and 5.9 wt%, respectively. The nature of the support had significant influence on the catalyst performance, more basic support gave a higher monomeric product yield and lower solid residue. Agarwal et al. (24) studied the solvent free hydrotreatment of Kraft lignin with sulfided Fe-based limonite catalysts. Reactions were carried out under 100 bars of initial hydrogen pressure, 4 h of reaction time and various reaction temperatures (350, 400 and 450°C). The highest yield of lignin oil, alkylphenolics and aromatics was achieved with a reaction temperature of 450°C with 33.7 wt%, 16.7 wt% and 4.1 wt%, respectively. Kloekhorst et al. (1) reported the solvent free hydrotreatment of Alcell lignin with Ru and Pd based catalysts. Reactions were carried in conditions of 100 bars of initial hydrogen pressure at 400°C and 4 h of reaction time. The highest yield of alkylphenolics and aromatics was achieved with Ru-TiO_2 which gave respectively 9.1 wt% and 2.5 wt%. A reaction network of the Kraft lignin depolymerization in solvent free conditions was proposed in our research group, which can be seen in Fig. 1.4. The unfavorable step in the reaction network is the reduction of aromatics to cyclohexanes and aliphatic compounds.

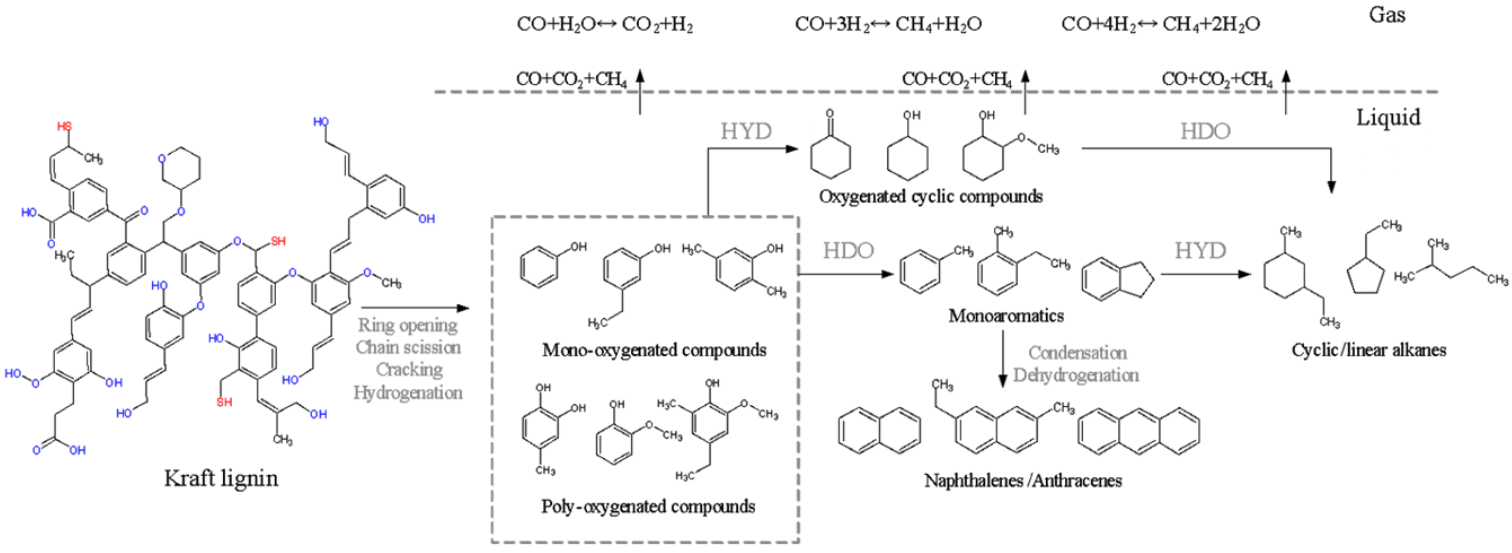

Fig. 1.4 Reaction network of Kraft lignin depolymerization

Traditional NiMo and CoMo catalysts were considered promising catalysts for Kraft lignin hydrotreatment because they require a sulfur source for activation, this is provided by Kraft lignin (9). Despite the sulfur in Kraft lignin, an additional sulfur source is necessary for activation, which can pollute the reaction product mixture. This drawback can be avoided by the use of noble metal catalysis, since these are not activated by sulfur. Also, char formation can be partially avoided by the use of noble metals since these reduce the mobility of carbon and therefore reduce the nucleation sites for coke formation (25). However, the high sulfur content of Kraft lignin represents a big challenge since it may cause sulfur poisoning in noble metal catalysts (26). In biomass conversion and deoxygenation, noble metals are widely used because of their efficient activation of H−H, C=O, C−O, and C−H bonds (27). In this research, Ru is applied as active metal since it has previously shown high activity in hydrotreatment of lignin. Kloekhorst et al. (1) showed that between Ru, Pd and Cu catalysts the Ru catalyst had the most promising results. Ru/TiO_2 showed a high degree of depolymerization and a high yield of alkylphenolics and aromatics. Yuan et al. (20) observed that between Ru and Ni catalysts, the Ru/C catalyst showed the most promising results and the highest degree of depolymerization. The excellent performance of Ru for lignin depolymerization can be explained by the oxophilic nature of Ru and high activity in hydrogen dissociation (28).

Kumar et al. (9) reported that the physico-chemical nature of the support can have a very strong effect on the performance of the catalyst, playing a key role in the reaction. Besides the traditional Al_2O_3, several other materials have been reported to be applicable as supports in hydrotreatment of lignin and lignin models compounds. Kong et al. (29) studied the conversion of enzymatic lignin to cyclic alkanes using Ni supported by Al_2O_3, SiO_2, TiO_2 and ZrO_2. The yield of liquid product compounds increased in the order of ZrO_2 < SiO_2 < TiO_2 < Al_2O_3. The authors observed that the liquid product yield increased linearly with the increasing trend of specific surface area of the catalysts. Higher surface area of support facilitates more accessible contact sites, and consequently shows a higher activity. Mao et al. (20) explored the hydrodeoxygenation of guaiacol (model compound) to phenolics using Au supported by Al_2O_3, SiO_2, anatase TiO_2, rutile TiO_2 and ZrO_2. The reaction with Au-ZrO_2 and Au-SiO_2 did not produce phenol. The yield of phenol increased in the order of Al_2O_3 < rutile TiO_2 << anatase TiO_2. Leo et al. (30) reported the hydrogenolysis of sorbitol to glycols using Ru supported by Al_2O_3, SiO_2, TiO_2 and ZrO_2. The highest conversion was achieved with the Ru-SiO_2 catalyst (96.1%) while the conversions of the Al_2O_3, TiO_2 and ZrO_2 catalysts were in the range of 73.9 – 85.8%. The highest selectivity towards glycols was achieved with the Ru-Al_2O_3 catalyst (19.1%) while the glycols yields of the SiO_2, TiO_2 and ZrO_2 catalysts were in the range of 4.9 – 5.2%. The high selectivity of Ru-Al_2O_3 towards glycols could be explained by the high surface concentration of acid sites and partially oxidized Ru species.

The regenerability and reusability of hydrotreatment catalysts is a key factor for the economic viability of the process, representing a great challenge, considering that the typically harsh conditions of hydrotreatment lead to catalyst deactivation generally due to coke formation. Catalyst deactivation was observed by Wildschut et al. (31) during the hydrotreatment of pyrolysis oil with supported Ru catalyst. A severe decrease of hydrogenation activity, oil yield and H/C ratio was observed after subsequent catalyst recycles. The catalysts were not regenerated in between cycles and catalyst characterization indicated that clustering of metal particles and coke deposition were the main cause for catalyst deactivation. Agarwal et al. (24) performed a recycling study of a Fe-based limonite catalyst for the hydrotreatment of Kraft lignin. The spent catalyst was regenerated by oxidative treatment prior to the second cycle. A significant decrease in BET surface area and a change in morphology was observed after regeneration. However, the regenerated catalyst still showed a substantial activity in Kraft lignin hydrotreatment.

In the case of Kraft lignin hydrotreatment, the following deactivation mechanisms will most likely occur: sulfur poisoning, coke fouling and thermal degradation (25).

The sulfur content in Kraft lignin may cause poisoning and deactivation of the catalyst. Sulfur shows strong chemisorption on the surface of the metal and blocks adsorption and reaction sites, as seen in Fig. 1.5. (32).

Köning et al. (33) showed that Ru can oxidize sulfur during regeneration in an oxygen rich atmosphere. After regeneration, no sulfur or sulfate species were observed on the Ru particles.

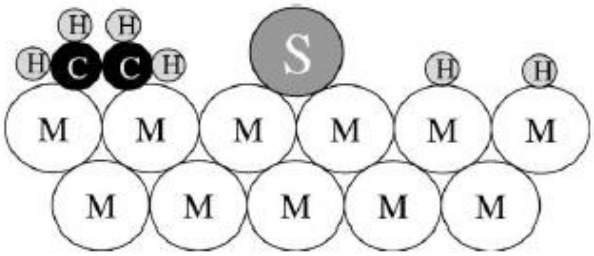

Fig. 1.5 Model of sulfur poising during ethylene hydrogenation (32)

Coke fouling occurs in lignin hydrotreatment by the deposition and condensation of polymerized hydrocarbons. Deactivation will take place by coke encapsulating the metal particle and by plugging micro- and mesopores. (25) The support of the catalyst can play a significant role in coke formation. Strong acid sites on the support are known to participate in condensation reactions. Catalyst regeneration will remove coke by combustion in oxidizing conditions. (34)

Thermal deactivation (sintering) of the catalyst is caused by loss of metal active sites by crystallite growth (agglomeration), loss of surface area by support collapse and loss of Ru by volatile RuO_x species. Agglomeration of metal particles is caused by atomic and crystallite migration over the support which results in collision and coalescence. The rate of metal particle growth increases exponentially with temperature. Also, the presence of water vapor, oxygen and weak metal support interactions increases the rate of metal particle growth. (25) The presence of water in combination with the harsh reaction conditions can cause the support/pore collapse due to a crystal phase transition, this decreases the supports surface area. Occurring of support/pore collapse during the hydrotreatment depends on the stability of the support during the reaction conditions. Another form of thermal degradation is the formation of volatile RuO_x species in oxidized conditions (regeneration). (34)

Scope of the research

In this research, the performance, reusability and regenerability of different supported Ru catalyst has been studied, on the hydrotreatment of Kraft lignin using a solvent-free approach. Five different catalysts with different physico-chemical properties have been prepared (via wet impregnation) and tested to determine the role of their support (Al_2O_3, SiO_2, TiO_2 and ZrO_2) and metal loading (0.3 and 1 wt% Ru).

A first set of reactions has been carried out at 450°C, 100 bars of initial hydrogen pressure and 4 h of reaction time. The performance of the catalysts were evaluated in terms of product distribution and composition. After that, the catalysts have been regenerated by means of coke combustion at 550°C for 4 h in air. A second reaction cycle has been carried out to gain insights on their reusability.

The fresh and regenerated catalysts have been characterized using several techniques (i.e. nitrogen physisorption, XRD and TEM) in order to be able to correlate their properties with their performance and understand the changes that take place on their structure during hydrotreatment and regeneration.

2. Material and Methods

In this chapter, the used materials and procedures for catalysts preparation, hydrotreatment reactions and the techniques used for reactions products analysis and catalyst characterization are explained. A detailed list of used materials and the specifications can be seen in appendix 1.

Catalyst preparation

The precursor used for impregnation was Ru-$(acac)_3$ (97%, purchased from Sigma Aldrich)and acetone (>95%, purchased from Boom B.V.) was used as the solvent. To prepare a batch of 6 g of catalyst with 1 wt% Ru loading, 5.94 g of support was suspended in the solvent and 0.24 g of metal precursor was added. The suspension was stirred for 4 h and afterwards the solvent was removed by evaporation and dried overnight at 60°C. To remove the organic component from the metal precursor, the catalyst was calcined. Calcination was performed in a tubular oven at 450°C for 4 h under nitrogen flow. Catalytic supports Al_2O_3, ZrO_2 (99%) and TiO_2 (99.9%) were purchased from Sigma Aldrich. The particle sizes of the supports are respectively 0.05-0.15 mm, 5 µm and <5 µm. The SiO_2 support was purchased from Silicycle and has a particle size of 40-63 µm.

Catalyst characterization

BET analysis at -196˚C was used to determine the specific surface area and pore structure, using a Micromeritics' ASAP2020 apparatus. Approximately, 100 mg of sample was used for each analysis and the sample was degassed for 6 h under vacuum at 150˚C prior to the analysis.

The crystallinity of the supports was determined with X-ray diffraction (Philips X-Pert Diffractometer) operated with a Ni β-filtered Cu Kα radiation, with a wavelength of 1.5406 Å. Data was collected with a step size of 0.02° with 1s per step, over a 2θ range of 2-80 degree.

The metal loading on the catalyst was analyzed with Inductively Coupled Plasma (ICP). The samples were dissolved by microwave treatment in 40% HF. The analysis was performed on a PerkinElmer Optima 7000 DV apparatus using a solid-state CCD array detector. Ar was used a purge gas and Yttrium (10 ppm) and scandium (10 ppm) as internal standards.

The morphology of the catalyst was studied by transmission electronic microscopy (TEM) using a Philips CM12 operated at an acceleration voltage of 120 kV. Samples were prepared by dispersion in ethanol and subsequently deposition on a mica grid coated with carbon.

Hydrotreatment reactions

The reactions were carried out in a batch autoclave (Parr instruments Co, 100 ml). During the reaction, the content was continuously stirred and heated by an electrical heating element surrounding the reactor. The heating element contains an entrance for the flowing of cooling water. Temperature and pressure were logged on a PC during the reaction. The reactor was filled with 15.0 g of Kraft lignin (purchased from Meadwestvaco Specialty Chemical) and 0.75 g of catalyst. Prior to the reaction, the autoclave was flushed 4 times with hydrogen to expel oxygen. After flushing, a leak test was performed at 180 bars of hydrogen at room temperature. When the pressure remains stable during the leak test, the pressure is set at 100 bars before the reactor is heated up to 450°C (10°C min^{-1}), and stirring starts. Time zero was set once 450°C was reached.

Once the reaction was finished, the reactor was cooled to room temperature. The pressure at room temperature is important to determine the amount of consumed hydrogen. The gas was collected in a Tedlar bag and analyzed with a Gas Chromatography. The liquid phase was pipetted out of the reactor and rapidly an oil and water layer would establish. A schematic overview of the reaction and reaction products is shown in Fig. 2.1.

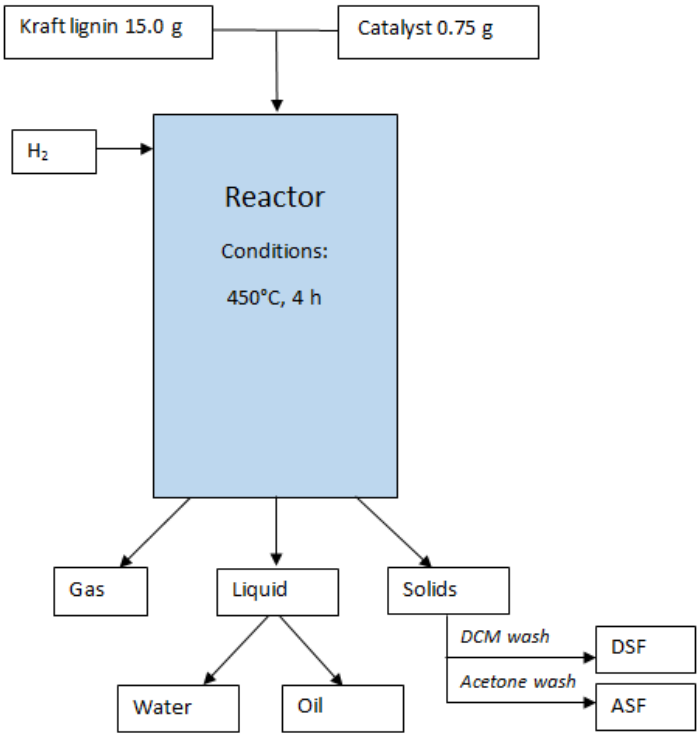

Fig. 2.1 Schematic overview hydrotreatment reactions

The remaining content in the reactor are the solid particles with heavy aromatic species adsorbed. The solids contain mainly catalyst and coke residue. The remaining products were separated by an extraction step. Solids were washed with Dichloromethane (DCM) and kept overnight. Then, solids were filtered off from the DCM fraction. DCM is highly volatile and evaporates overnight, only the DCM soluble fraction (DSF) would remain. The solids in the filter were washed also with acetone. Evaporation of acetone results in the acetone soluble fraction (ASF). DCM and acetone were purchased from Boom B.V.. After the reactions, the yields of the products and the mass balance were calculated using equations 1 and 2:

$$Product\ yield\ (\%) = \frac{Product\ wt.}{Initial\ lignin\ wt.} \times 100 \quad (1)$$

$$Mass\ balance\ (\%) = \frac{Sum\ of\ the\ wt.of\ all\ products}{Initial\ lignin\ wt.} \times 100 \quad (2)$$

Product analysis techniques

Gas samples were analyzed with Hewlett Packard 5890 Series II using a Porablot Q Al2O3/Na2SO4 column and a molecular sieve (5 A) column. The oven was heated from 40°C to 90°C at 20 °C min^{-1}, the temperature of the injector was set at 150 °C and the detector temperature was set at 90 °C. A reference gas was used to identify the peaks by retention time (55.19% H_2, 19.70% CH_4, 3.00% CO, 18.10% CO_2, 0.51% ethylene, 1.49% ethane, 0.51% propylene and 1.5% propane, purchased from Westfalen).

Lignin oil samples were analyzed with GC x GC-FID using a trace GC x GC from Interscience equipped with two columns (RTX-1701 capillary column and an Rxi-5Sil MS column) in combination with an FID detector. A dual jet modulator was applied to trap the samples by freezing with CO_2 (purchased from Linde). The injector and FID detector operated at 250 °C. After 5 minutes, the oven temperature is heated from 40°C to 250°C at 3 °C min^{-1}, at 40 °C the pressure was set at 70kPa. Helium was used as the carrier gas (purchased from Linde) and modulation time was 6 seconds.

Lignin oil samples were analyzed with GC-MS-FID using a Quadruple Hewlett Packard 6890 MSD in combination with a Hewlett Packard 5890 GC using a sol-gel capillary column (60 m × 0.25 mm i.d. and a 0.25 µm). After 5 minutes, the oven temperature is heated from 40°C to 250°C at 3 °C min^{-1} and held at 250 °C for 10 minutes. The injector temperature was set at 250 °C.

For both the GC-MS-FID and GC x GC FID analysis the samples were diluted in THF (tetrahydrofuran), DBE (di-*n*-butylether) as an internal standard.

Lignin oil, DSF and ASF samples were analyzed with GPC to obtain their molecular weight distributions. Prior the analysis, the samples were dissolved in THF and a few drops of toluene were added as a flow marker. The samples were analyzed using a HP1100 equipped with three MIXED-E columns (300 × 7.5 mm PL gel 3 µm) in combination with a GBC LC 1240 RI detector. The injection volume is 20 µl, with a sample concentration of 1 mg ml^{-1}. THF was used as eluent at a flow rate of 1 ml min^{-1}. The temperature of the column was held at 40°C. For data processing, PSS WinGPC Unity software from Polymer Standards Service was used.

Lignin oil samples were analyzed with HSQC NMR using an Agilent 400 MHz spectrometer at 25 °C. Approximately 0.2 g of liquid sample was diluted in 1 g of dimethyldisulfoxide-d6 (DMSO). A standard pulse sequence HSQC program with a spectral width of 160 ppm, 8 scans, 1024 increments was used to obtain the spectra. The obtained data were processed using MestRenova software.

Lignin oil and solid samples were analyzed by means of elemental analysis. The C, H, N and S content was determined using a Euro Vector 3400 CHN-S, the O content was determined by the difference.

The water samples were analyzed with total organic carbon (TOC) using a Shimadzu TOC–VCSH TOC analyzer with an OCT-1 sampler port.

Lignin oil samples were analyzed for their water content with Karl Fischer titration using a Metrohm Titrino 758 titration device. The measurements were performed in duplicate and a small amount of sample (ca. 0.03-0.05 g) was used. The isolated glass chamber contains Hydranal® (Karl Fischer Solvent, Riedel de Haen). Karl Fischer titrant Composit 5K (Riedel de Haen) was used for titration.

3. Results

In this chapter, the results of catalyst preparation, hydrotreatment reactions, product analysis and catalyst characterization are provided. The Ru loading of the catalysts were determined with ICP after preparation. The hydrotreatment of Kraft lignin was performed with both fresh and regenerated catalysts (as divided in the coming section). After the reaction, the lignin oils were analyzed with GC x GC-FID, GPC, GC-MS-FID, NMR and elemental analysis. The fresh and regenerated catalysts were characterized with XRD, BET and TEM analysis.

Catalyst preparation

After preparation, the catalysts were analyzed with ICP to determine the Ru loading. The results can be seen in Table 3.1.

Table 3.1 Overview of Ru loading on fresh catalysts in wt%

Catalyst	Fresh
1%Ru-Al_2O_3	1.0
1%Ru-SiO_2	0.9
1%Ru-TiO_2	1.2
0.3%Ru-TiO_2	0.3
0.3%Ru-ZrO_2	0.3

5 catalysts with 0.3 and 1 wt% Ru loading were prepared. In case of the 0.3 wt% Ru catalysts, the exact Ru loadings were achieved. A slight variation in Ru loadings were observed for the 1 wt% Ru catalysts, with a range of 0.9-1.2 wt%. The loadings were rounded up and the catalysts were compared as 1%Ru catalysts.

Catalytic hydrotreatment

A first series of catalytic hydrotreatment reactions with Kraft lignin were carried out with fresh Ru catalysts with various supports (Al_2O_3, SiO_2, ZrO_2 and TiO_2) and various metal loadings (0.3 and 1 wt%). After the reaction, the catalysts were regenerated and used for a second cycle of Kraft lignin hydrotreatment. Prior to the second cycle, the catalyst had endured harsh conditions during hydrotreatment and regeneration. To determine to what extent hydrotreatment and/or regeneration affects the physico-chemical properties of the catalyst, a sample of fresh catalyst was also subjected to regeneration conditions and used for characterization and comparison.

Fresh catalysts (1st reaction cycle)

The product distribution (lignin oil, DSF, ASF, water, gas and solid phases) and the mass balances obtained on the first reaction cycle using fresh catalysts are presented in Table 3.2.

Table 3.2 Product distributions and mass balances for Kraft lignin hydrotreatment using the fresh catalysts

Catalyst	Oil (%)	DSF (%)	ASF (%)	Water (%)	Gas (%)	Solids (%)	Mass balance
1%Ru-Al_2O_3	35.9	3.8	1.6	20.9	14.9	21.7	93.3
1%Ru-SiO_2	37.5	4.4	1.5	21.2	15.5	17.4	91.6
1%Ru-TiO_2	39.6	4.0	1.0	20.2	14.8	19.1	93.8
0.3%Ru-TiO_2	39.4	4.3	2.1	20.2	15.3	18.6	93.6
0.3%Ru-ZrO_2	38.1	4.0	1.2	20.5	16.0	18.6	93.1

The liquid phase of the reactions products was separated in a lignin oil and water layer with yields of 35-40 wt% and 20-21 wt%, respectively. The gaseous and solids phase were in the range of 14-16 wt% and 17-22 wt%, respectively. Washing the solids with DCM and acetone gave DSF and ASF yields in the range of 3-5 wt% and 1-2 wt%. Good mass balance closures were achieved (>90%), complete mass balance closure is impossible due to product losses during work-up.

Despite the various supports and metal loadings, the difference in the fresh catalysts performance was not significant with lignin oil yields in between 35-40 wt%. The most active catalyst regarding lignin oil yield was the 1%Ru-TiO_2 catalyst with 39.6 wt% and interestingly, the lignin oil yield for the 0.3%Ru-TiO_2 catalyst was similar (39.4 wt%) due to the high activity of Ru for Kraft lignin hydrotreatment. The results in table 3.2 indicate that difference in support and metal loading does not significantly affect the activity of the fresh catalysts. In comparison with a Fe-based limonite catalyst, applied with the same reaction conditions by Agarwal et al. (24), all 5 catalysts showed a higher lignin oil yield than the limonite catalyst (33.7 wt%).

GPC

The molecular weight distribution is determined with GPC analysis as shown in Fig 3.1 and 3.10. Fig 3.1 shows the molecular weight distribution of Kraft lignin, lignin oil, DSF and ASF from the reaction using the fresh 1%Ru-TiO_2 catalyst. The average M_w of Kraft lignin is roughly 1000 g mol^{-1}, the M_w was significantly decreased by hydrotreatment, with the average M_w of lignin oil, DSF and ASF of respectively 200, 210 and 215 g mol^{-1}. The lower M_w of lignin oil compared with DSF and ASF is observed in the GPC chromatogram in Fig 3.1. In comparison with the lignin oil peak, the DSF and ASF peaks are wider and show a slightly higher M_w which indicates that the monomeric compounds in DSF and ASF are heavier than the compounds in the lignin oil.

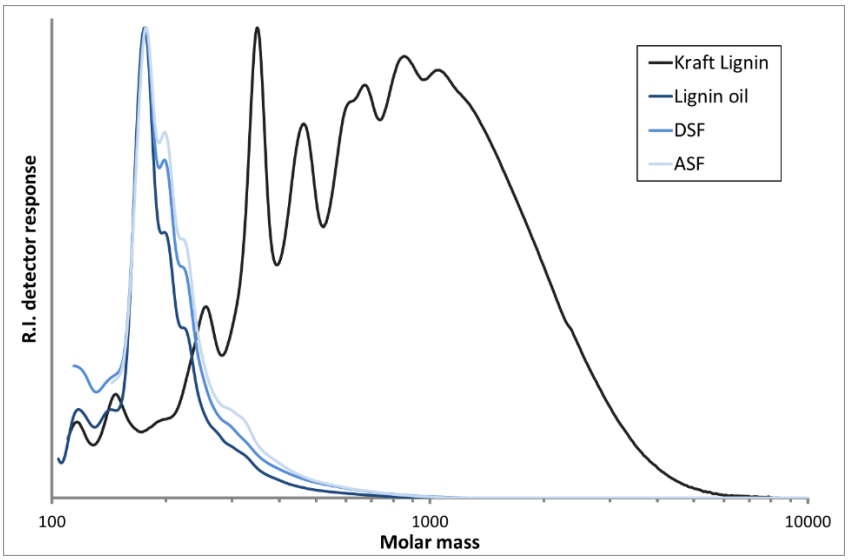

Fig. 3.1 Molecular weight distribution of Kraft lignin, lignin oil, DSF and ASF from the reaction using the 1% Ru-TiO_2 catalyst

Van Krevelen plot

The elemental composition of the lignin oils and Kraft lignin were determined by elemental analysis, the results are shown in appendix 2. From this information, the atomic O/C and H/C ratios were calculated, and presented in the form of a van Krevelen plot (Fig 3.2).

The extent of hydrodeoxygenation by catalytic hydrotreatment is clearly observed in terms of O/C ratio with a decrease from 0.36 in Kraft lignin to 0.06-0.07 in the lignin oils. The reduction of H/C ratio after the catalytic hydrotreatment occurred in a less extent. The H/C ratio of Kraft lignin is 1.15 and is reduced to 1.06-1.08 in the lignin oils.

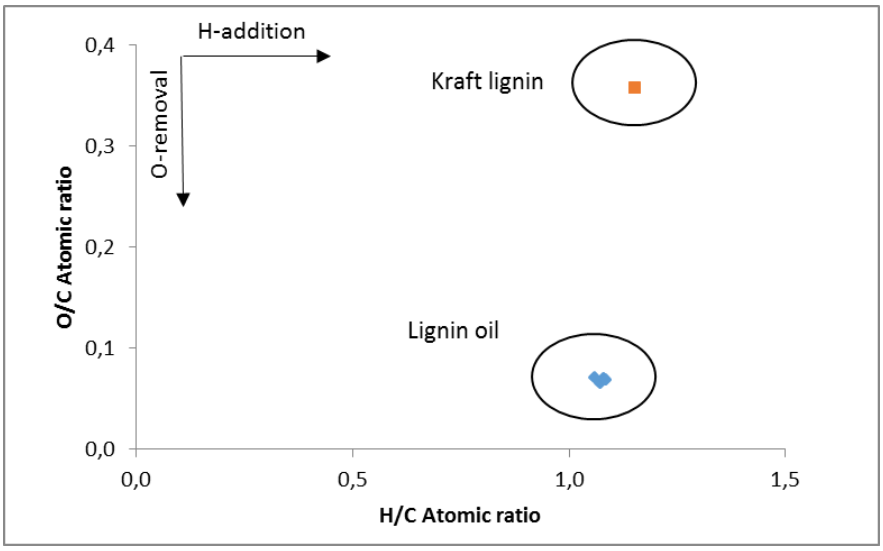

Fig. 3.2 Van Krevelen plot of lignin oil and Kraft lignin

Chemical composition of lignin oil and DSF

An important aspect of the lignin oil is the yield of monomers, which is analyzed with GC x GC-FID. Fig. 3.3 shows a typical chromatogram obtained for the analysis of lignin oil, and also the different chemical groups which can be identified and grouped via this technique, such as: alkylphenolics [8], catecholics [9], guaiacolics [7], alkanes [2], aromatics [3], ketones [5], cyclohexanes [1] and naphtalenes [4].

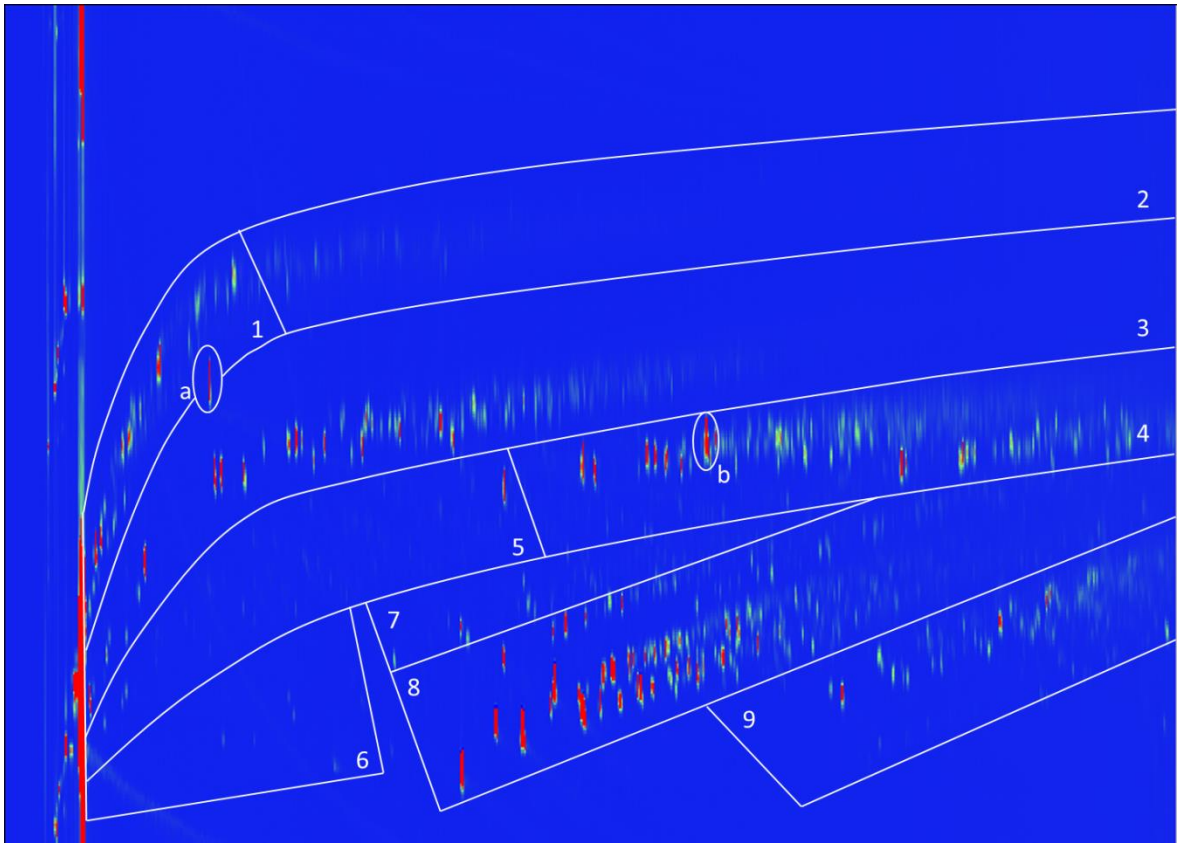

Fig. 3.3 GC x GC chromatogram of the lignin oil from the reaction using 1%Ru-TiO_2 catalyst

Table 3.3 shows the quantification of the monomeric product yield from hydrotreatment reactions using fresh catalysts. The main chemical groups that are identified from the lignin oil are alkylphenolics and aromatics. The 1%Ru-TiO_2 catalyst showed the highest yield of alkylphenolics (16.1 wt%) and aromatic (4.5 wt%) on lignin intake while similar yields were found for the 0.3%Ru-TiO_2 catalyst (15.9 wt% alkylphenolics and 3.8 wt% aromatics). The total monomer yield from the reaction using 1% and 0.3%Ru-TiO_2 catalysts were respectively 31.3 and 29.1 wt%. The 1%Ru-Al_2O_3 catalyst showed the lowest activity in terms of alkylphenolic (14.5 wt%), aromatic (4.3 wt%) and monomer (27.8 wt%) yields.

Table 3.3 Monomeric product yield (wt% on lignin intake) from the reactions using fresh catalysts

	1%Ru-Al_2O_3	1%Ru-SiO_2	1%Ru-TiO_2	0.3%Ru-TiO_2	0.3%Ru-ZrO_2
Alkylphenolics	14.5	14.7	16.1	15.9	15.1
Catecholics	1.6	2.4	2.5	1.7	2.2
Guaiacolics	0.7	0.9	1.3	1.1	1.1
Alkanes	0.3	0.5	0.3	0.4	0.4
Aromatics	4.3	3.7	4.5	3.8	3.8
Ketones	0.3	0.3	0.3	0.3	0.3
Cyclohexanes	3.0	2.8	2.9	2.6	2.9
Naphthalenes	3.2	3.1	3.4	3.3	3.4
Monomer yield %	27.8	28.4	31.3	29.1	29.1

Despite the low metal loading of the catalyst, the results were more promising than preceding experiments with commercial Ru catalyst (5 wt% metal loading), performed in our group using the same reaction procedure and conditions. The outcome of these experiments resulted in 5%Ru/C being the most active catalyst of the commercial Ru catalysts, with yields of 31.5 wt% lignin oil, 14.7 wt% alkylphenolics and 5.3 wt% aromatics. This catalyst shows less activity in comparison with the 1 and 0.3 wt% catalysts regarding oil yield, shown in Table

3.3 (lignin oil yield 35.9 - 39.6 wt%). The yields of alkylphenolics and aromatics between the 5%Ru/C catalyst and the 0.3% and 1% catalysts (alkylphenolics 14.5 – 16.1 wt% and aromatics 3.7 – 4.5 wt%) were comparable.

The DSF was also analyzed in terms of chemical composition, to explore the possibilities for DSF as a source for biobased chemicals. Table 3.4 shows the relative concentrations of the different monomeric products in DSF and lignin oil from the reaction with the 1%Ru-TiO_2 catalyst. The GC x GC-FID chromatogram corresponding to the DSF from the 1%Ru-TiO_2 reaction is shown in Fig 3.4.

Table 3.4 Relative concentration monomeric product (wt% in lignin oil and DSF) obtained using the 1%Ru-TiO_2 catalyst

1%Ru-TiO_2	Concentration in oil/DSF	
	Oil	**DSF**
Alkylphenolics (8)	41.0	36.9
Catecholics (9)	6.2	1.2
Guaiacolics (7)	3.4	2.4
Alkanes (2)	0.9	0.0
Aromatics (3)	11.3	1.9
Ketones (5)	0.6	0.4
Cyclohexanes (1)	6.9	0.0
Naphthalenes (4)	8.9	13.5

The concentration of naphtalenes in the DSF is higher than in the lignin oil and concentrations of monomeric compounds such as, catecholics, alkanes, aromatics and cyclohexanes are significantly lower in the DSF. This is also observed in Fig 3.4, where the regions with catecholics [9], alkanes [2], aromatics [3] and cyclohexanes [1] show less peaks in comparison with Fig 3.3. In general, the monomeric compounds in the DSF have a higher molecular weight than the monomeric compounds in lignin oil, which was also observed in the GPC analysis.

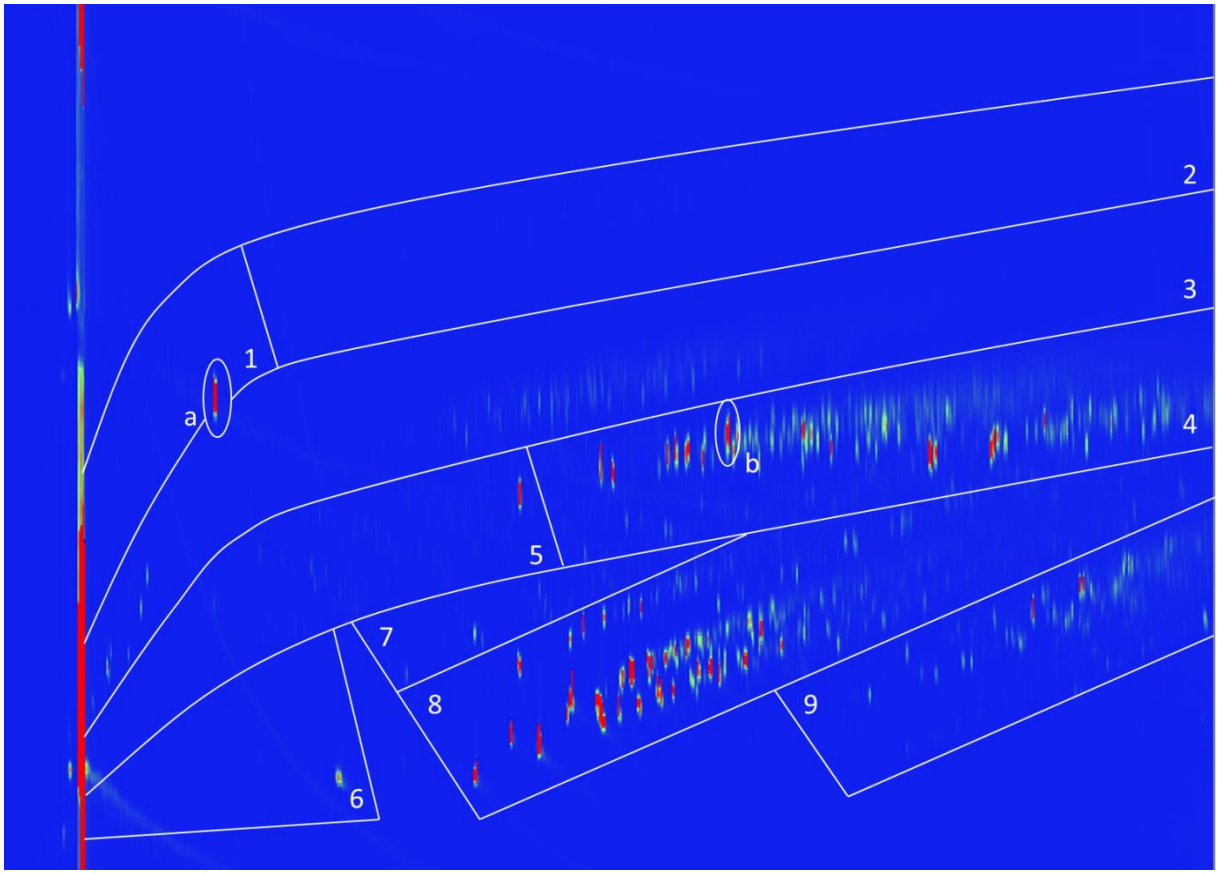

Fig. 3.4 GC x GC chromatogram of the DSF from the reaction with 1%Ru-TiO_2 catalyst

The large number of peaks in the GC x GC-FID analysis in Fig 3.3 and 3.4 show that the lignin oil and the DSF contain a large variety of compounds. With GC-MS-FID, some specific compounds in lignin oil and DSF are determined, as is shown in Fig 3.5, correspondingly to the lignin oil and DSF samples obtained using the 1%Ru-TiO_2 catalyst. The peaks in the DSF analysis were mainly found in the region of alkylphenolics and heavy aromatics while peaks in the lignin oil analysis were mainly found in the region of aliphatics, aromatics and alkylphenolics. The most abundant compounds in the lignin oil were: methylcyclohexane [1], toluene [2], phenol [8], 2-methylphenol [9] and 4-methylphenol [11]. The GC-MS-FID analysis shows that when lignin oil and DSF are compared, DSF contains compounds with higher average M_w, this was also observed in the GPC and GC x GC-FID analysis.

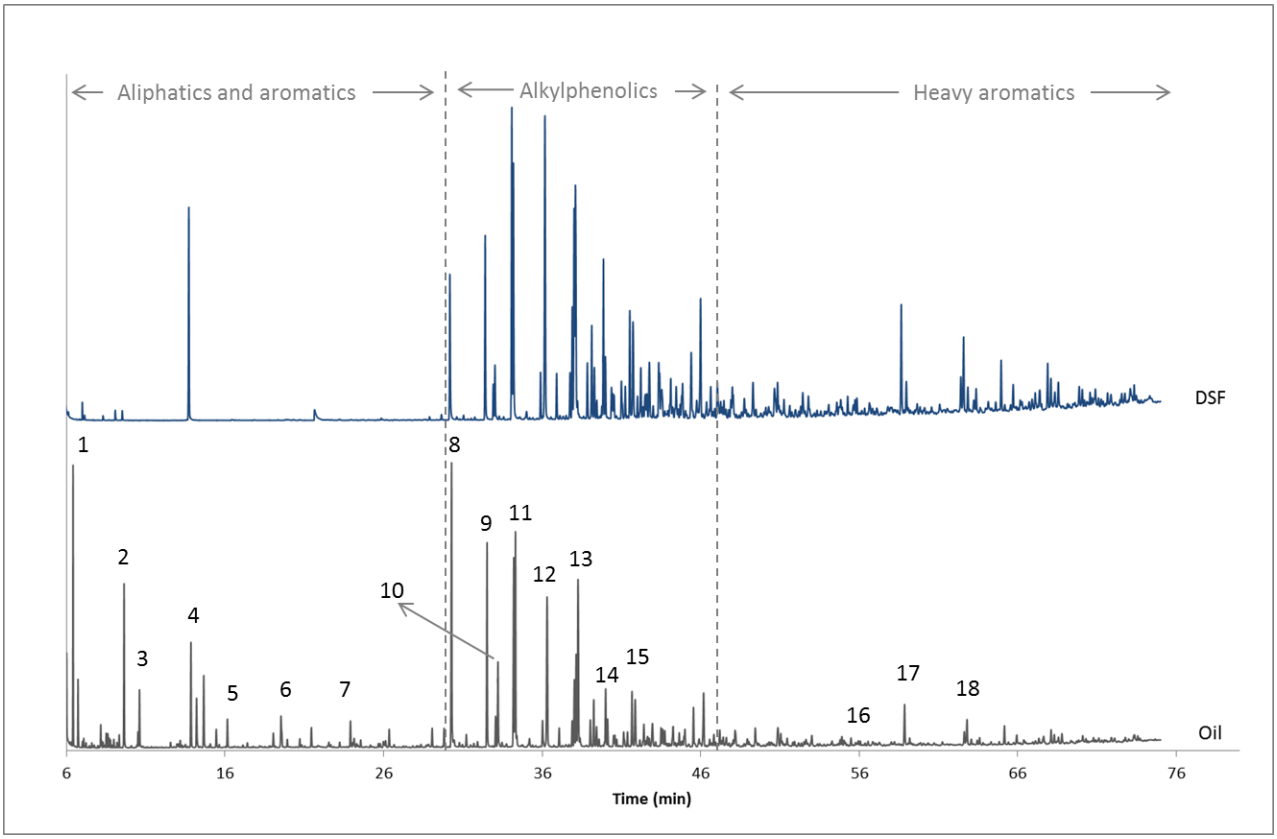

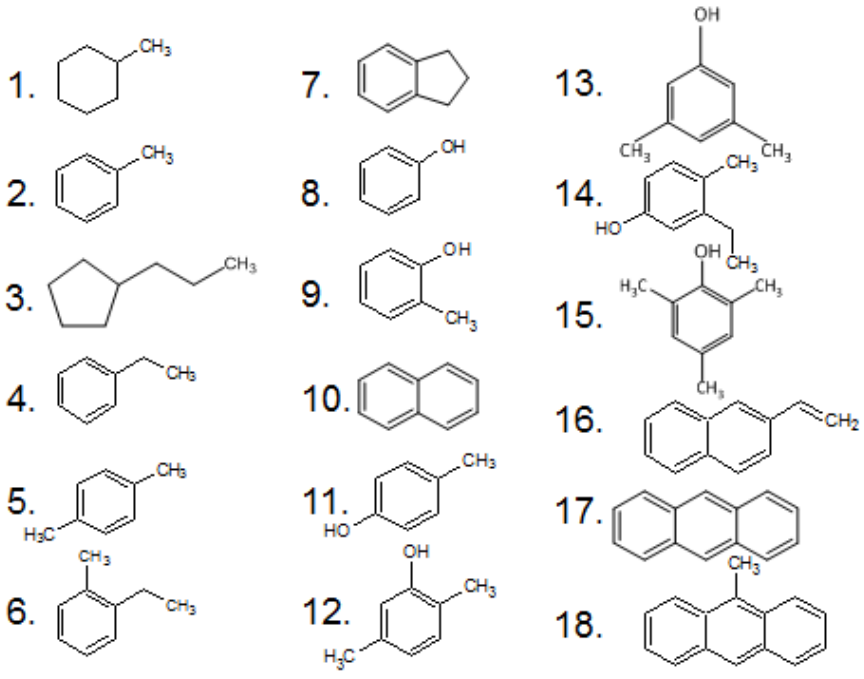

Fig. 3.5 GC-MS-FID chromatogram of lignin oil and DSF from the reaction with fresh 1%Ru-TiO_2 catalyst

HSQR NMR

HSQR NMR has proven to be one of the most powerful tools for analyzing the structural changes that take place during lignin depolymerization. The NMR spectra of Kraft lignin and the lignin oil of the 1%Ru-TiO_2 reaction are shown in Fig 3.6 a and b. The NMR spectra of lignin oil from reactions with other catalysts showed no significant differences and are not depicted.

The spectra of Kraft lignin shows the typical linkages common to most lignins (β-0-4γ, β-5γ, β-βγ, β-0-4α, β-0-4β and β-5α) between the aromatic monomers. The NMR spectra of the lignin oil shows that the linkages have been cleaved after depolymerization, and only two main regions were observed: the aliphatic and aromatic region. The peaks in the aliphatic regions show substituted alkylphenolics and overreduced cyclohexanes and alkenes. The peaks in the aromatic region show the aromatic compounds which are also observed in GC x GC-FID and GC-MS FID.

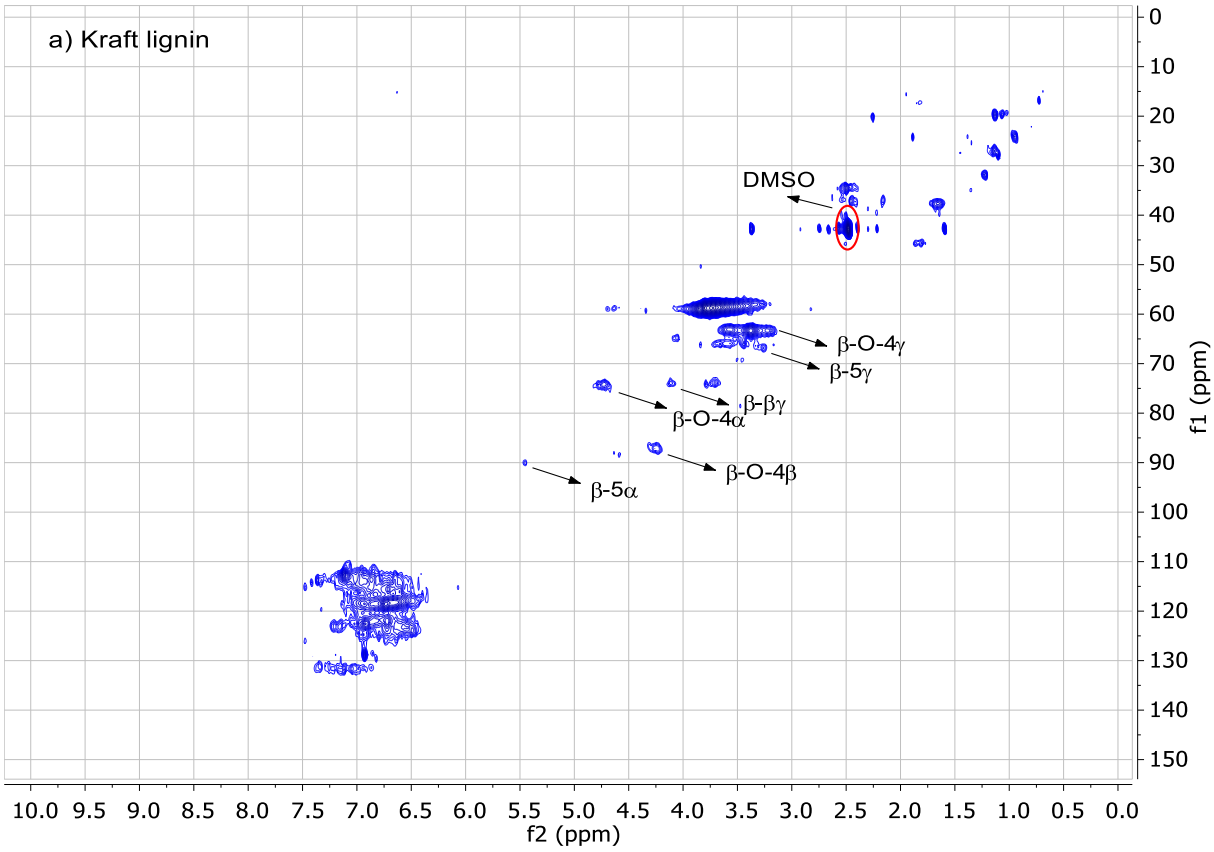

Fig. 3.6 a) NMR spectra of Kraft lignin

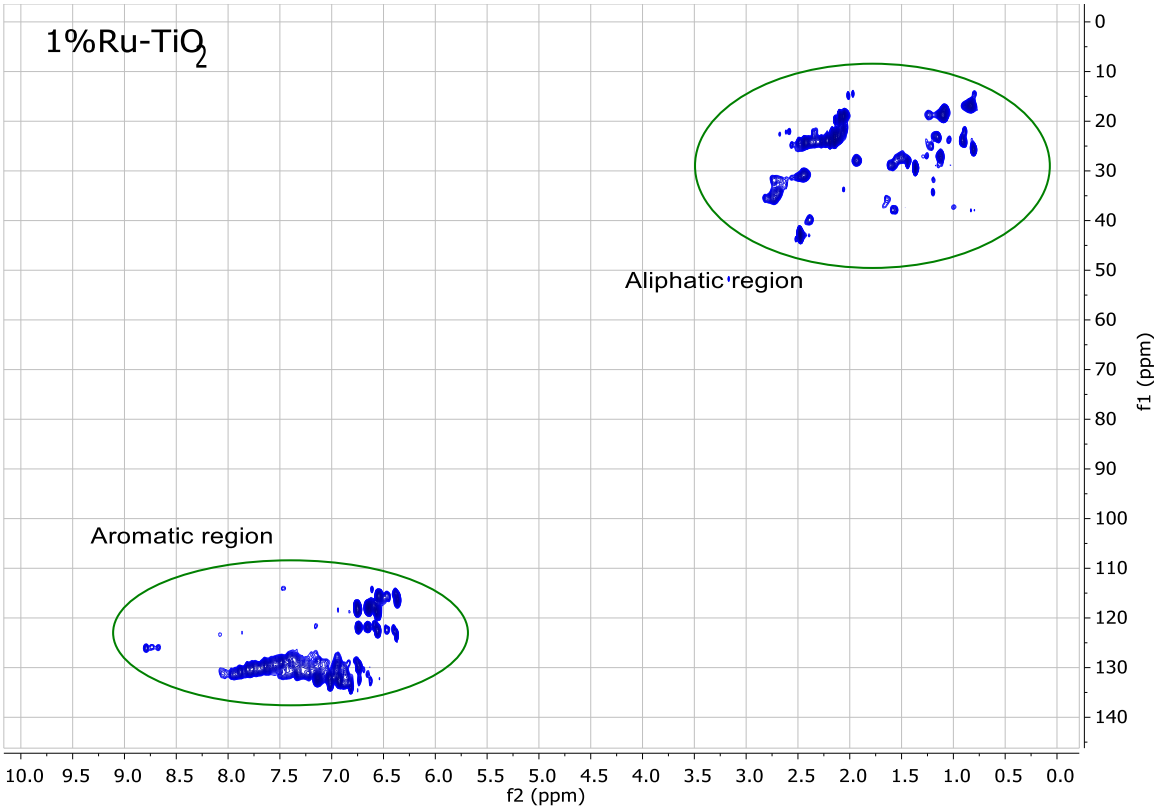

Fig. 3.6 b) NMR spectra of lignin obtained for the reaction with 1%Ru-TiO_2 catalyst

Regenerated catalysts (2nd reaction cycle)

After the first reaction cycle with fresh catalysts, the solids were obtained from the reactor and washed with DCM and acetone. These solid products contain the catalyst covered (encapsulated) in coke, which has been formed due to repolymerization reactions during the hydrotreatment. This leads to deactivation of the catalyst because the active sites are blocked by coke formation. To remove the coke, the catalyst is regenerated by means of coke combustion in a tubular oven at 550°C for 4h in air.

A second series of reactions has been performed to determine the activity of the regenerated catalysts. The results corresponding to the product distributions and mass balances for the second series of hydrotreatment reactions are presented in Table 3.5.

Table 3.5 Product distributions and mass balances for Kraft lignin hydrotreatment using regenerated catalysts

Catalyst	Oil (%)	DSF (%)	ASF (%)	Water (%)	Gas (%)	Solids (%)	Mass balance
1%Ru-Al_2O_3	30.6	2.9	0.5	21.4	14.8	25.1	91.9
1%Ru-SiO_2	27.5	2.2	0.4	20.9	10.8	28.3	87.4
1%Ru-TiO_2	36.7	4.3	2.4	20.4	17.5	20.0	94.5
0.3%Ru-TiO_2	27.9	4.5	0.7	20.7	19.0	29.0	96.7
0.3%Ru-ZrO_2	26.3	2.8	0.7	21.2	10.9	28.5	87.0

A significant decrease in lignin oil yield was observed, except when the 1% Ru-TiO_2 catalyst was used, this showed a decrease in lignin oil yield from 39.6 to 36.7 wt%. When the other regenerated catalyst were used, lignin oil yields in the range of 26-31 wt% were obtained, while lignin oil yields in the range of 35-40 wt% were obtained during hydrotreatment using fresh catalysts. An overview in change of lignin oil yield between fresh and regenerated catalysts can be seen in Fig 3.7. When the regenerated 1% and 0.3% Ru-based catalysts were

compared with the regenerated Fe-based limonite catalyst (applied by Agarwal et al. (24) in the same reaction conditions) it was concluded that the Ru-based catalysts show a larger oil yield decrease. Regeneration of the limonite catalysts only led to a lignin oil yield decrease from 34 wt% to 33 wt%. In case of the Ru-based catalysts, an increase in solids yields was observed from 17-22 wt% when fresh catalyst were used to 20-29 wt% when regenerated catalysts were used. The gaseous and water phase yield was in the range of 10-19 wt% and 20-22 wt%. The yield of dichloromethane soluble fraction (DSF) and acetone soluble fraction (ASF) was in the range of 2-5 wt% and 0.4-3 wt%. The mass balance closures (>85%) were satisfactorily.

The decrease in lignin oil yield and increase in solid yield are clear signs of catalyst deactivation. During the hydrotreatment of pyrolysis oil, Wildschut et al. (31) observed that the catalyst deactivated by metal particle clustering and coke deposition. The cause for the decrease in lignin oil yield might be due to metal particle clustering, coke deposition cannot be the cause due to regeneration.

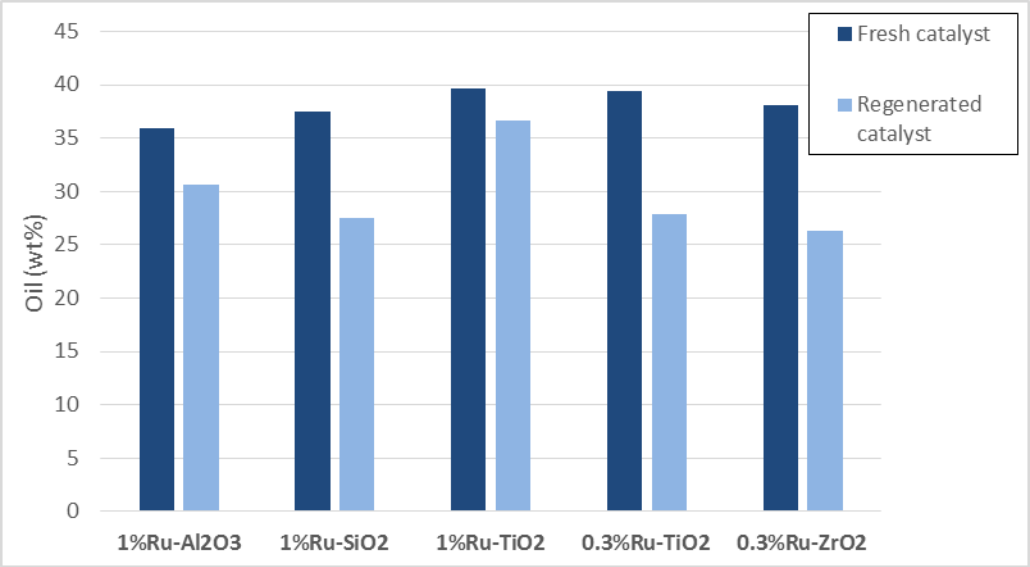

Fig. 3.7 Comparison in lignin oil yield between fresh and regenerated catalyst

GPC

The deactivation of the regenerated catalysts is clearly observed by a decrease in lignin oil yield, shown in Fig. 3.7. It was expected that deactivation would decrease the degree of lignin depolymerization. However, this could not be observed by the M_w of the lignin oil from reactions with fresh and regenerated catalysts, shown in Table 3.6. The M_w of the lignin oil from reactions with fresh catalysts is within the range of 200-205 g mol^{-1}, the lignin oil from reactions with regenerated catalysts is within the range of 190-200 g mol^{-1}. Instead of a decrease in depolymerization, the lignin oil from regenerated catalysts shows a slightly lower M_w, this indicates that the degree of depolymerization does not decrease when regenerated catalysts were used. However, the quantity of depolymerization did decrease, observed by the decrease in lignin oil yield. Therefore, using the regenerated catalysts leads to lower lignin oil yield with similar molecular weights.

Table 3.6 Overview of M_w lignin oil, DSF and ASF

Catalyst	Average Mw g mol^{-1}		
Fresh	**Oil**	**DSF**	**ASF**
1%Ru-Al_2O_3	200	210	215
1%Ru-SiO_2	200	205	205
1%Ru-TiO_2	200	210	215
0.3%Ru-TiO_2	200	225	220
0.3%Ru-ZrO_2	205	225	210
Regenerated	**Oil**	**DSF**	**ASF**
1%Ru-Al_2O_3	195	220	225
1%Ru-SiO_2	195	230	250
1%Ru-TiO_2	200	215	210
0.3%Ru-TiO_2	195	210	220
0.3%Ru-ZrO_2	190	200	220

Van Krevelen plot

The elemental composition of the lignin oils from reactions with fresh and regenerated catalysts were determined by elemental analysis. The results are presented in the form of a van Krevelen plot shown in Fig. 3.8 and in appendix 2.

The hydrodeoxygenation of Kraft lignin is more significant when fresh catalysts are used than when regenerated catalysts are used. The O/C ratio of Kraft lignin is 0.36 and was reduced to 0.06-0.07 in the lignin oils from fresh catalysts and 0.07-0.2 in the lignin oils from regenerated catalysts. The most decrease in hydrodeoxygenation was observed with the lignin oil from the regenerated 1%Ru-SiO_2 catalyst with an O/C ratio of 0.2. The reduction of the H/C ratio occurred in a less extent when regenerated catalysts were used. The H/C ratio of Kraft lignin is 1.15 and was reduced to 1.06-1.08 in the lignin oils from fresh catalysts and 1.09-1.22 in the lignin oils from regenerated catalysts.

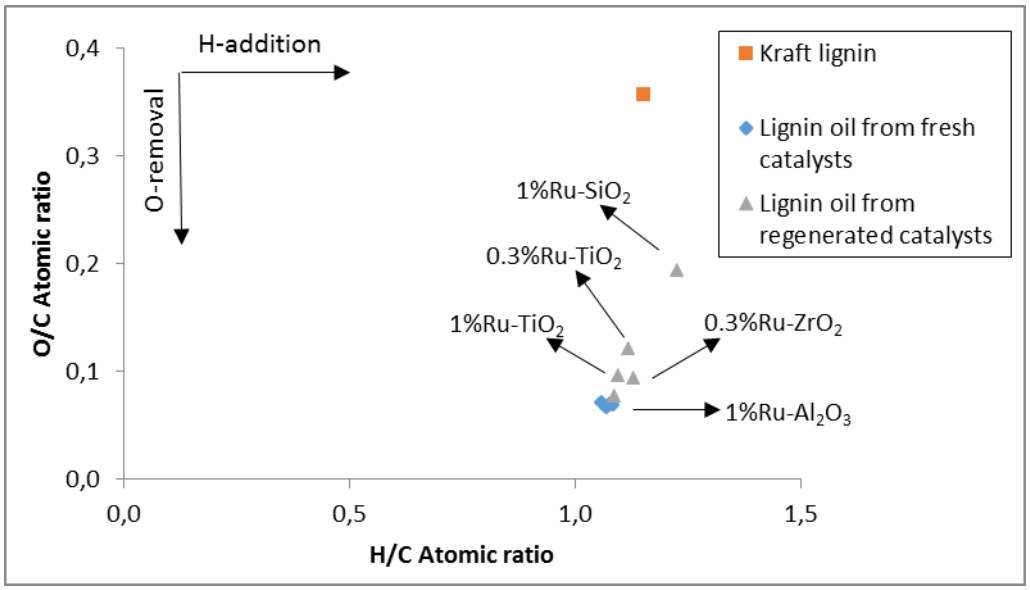

Fig. 3.8 Van Krevelen plot for the lignin oils obtained using the fresh and regenerated catalysts

Chemical composition of lignin oil

From the reactions with regenerated catalysts, the yields of monomeric products based on the lignin intake are presented in Table 3.7.

Table 3.7 Monomeric product yield (wt% on lignin intake) as obtained from the reactions using regenerated catalysts

	1%Ru-Al_2O_3	1%Ru-SiO_2	1%Ru-TiO_2	0.3%Ru-TiO_2	0.3%Ru-ZrO_2
Alkylphenolics	14.3	10.8	16.2	13.1	13.3
Catecholics	1.4	1.0	2.5	1.5	1.7
Guaiacolics	0.4	0.2	2.9	0.3	0.6
Alkanes	0.8	0.1	0.3	0.2	0.2
Aromatics	3.2	2.8	4.7	3.0	3.5
Ketones	0.4	0.4	0.3	0.6	0.6
Cyclohexanes	1.8	1.8	0.8	1.4	1.2
Naphthalenes	2.3	1.7	1.4	2.0	2.6
Monomer yield %	24.6	18.9	29.1	22.0	23.7

The most abundant chemical groups that are identified from the lignin oil by GC x GC-FID are alkylphenolics and aromatics. The 1%Ru-TiO_2 catalyst showed the highest alkylphenolic (16.2 wt%) and aromatic (4.7 wt%) yield, this was similar to the yields obtained in fresh conditions (alkylphenolics 16.1 wt% and aromatics 4.5 wt%). In fresh conditions, the yields of the 0.3%Ru-TiO_2 catalyst were comparable to the yields of the 1%Ru-TiO_2 catalyst, this was not repeated in regenerated conditions, since the total monomer yield of the 0.3%Ru-TiO_2 catalyst decreased from 29.1 wt% to 22.0 wt%. A similar effect was observed for the other catalysts, a significant decrease in monomer yield after regeneration of the catalyst.

Table 3.7 shows the monomeric product yield based on the lignin intake, not the relative concentrations of the monomeric products in the lignin oil. The relative concentrations in the lignin oil can be seen in appendix 3. Herein, is observed that the relative concentration of monomeric products in the lignin oil does not decrease when regenerated catalysts are used. Therefore, the decrease of monomeric product yield based on the lignin intake is a direct result of the decrease in lignin oil yield. The same observation was made from the GPC analysis of the lignin oil from the regenerated and fresh catalysts, since the M_w did not increase when regenerated catalysts were used.

Recycling study 1%Ru-TiO_2

After regeneration, the 1%Ru-TiO_2 catalyst was the least deactivated. The regenerability of this catalyst was further explored with a recycling study and a third reaction cycle. The corresponding product yield of the different reaction cycles are shown in Table 3.8 and Fig 3.9.

Table 3.8 Product distributions and mass balances for Kraft lignin hydrotreatment using 1%Ru-TiO_2 catalyst for 3 cycles

1%Ru-TiO_2	Oil (%)	DSF (%)	ASF (%)	Water (%)	Gas (%)	Solids (%)	Mass balance
Cycle 1	39.6	4.0	1.0	20.2	14.8	19.1	93.8
Cycle 2	36.7	4.3	2.4	20.4	17.5	20.0	94.5
Cycle 3	31.1	7.6	1.3	21.2	11.9	24.3	88.4

After cycle 1, 2 and 3, the catalyst deactivation is observed by a decrease in lignin oil yield from 39.6, to 36.7, to 31.3 wt% and increasing DSF yields. The monomeric compounds in DSF are heavier than the monomeric compounds in lignin oil, this was observed in GPC analysis in Fig. 3.1 and GC-MS-FID analysis in Fig. 3.5. Hence, a milder depolymerization of lignin due to catalyst deactivation, yields an increase in DSF. Another result of catalyst deactivation was the increase in coke formation (increasing solid yield).

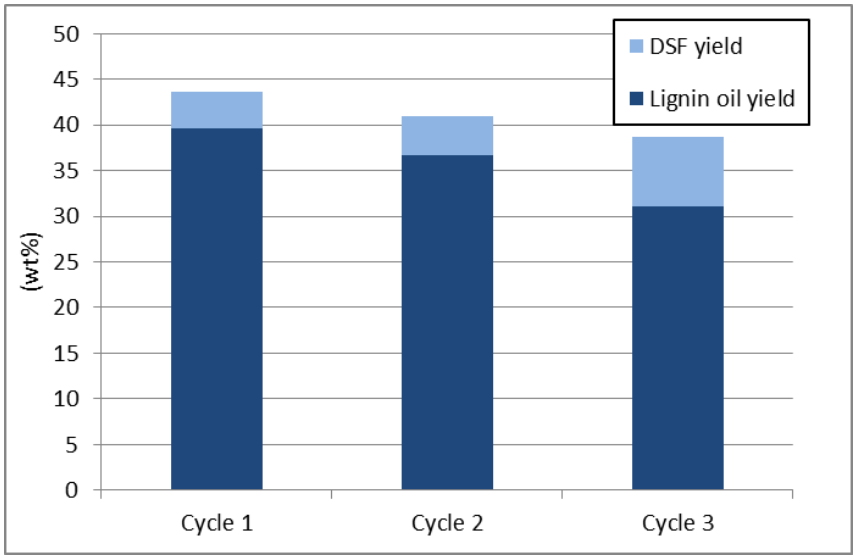

Fig. 3.9 Lignin oil and DCM yield after 3 cycles with 1%Ru-TiO_2

From the 1%Ru-TiO_2 recycling reaction, the yields of monomeric products based on the lignin intake are presented in Table 3.9. While cycle 1 and 2 show similar yield of alkylphenolics (16.1 and 16.2 wt%) and aromatics (4.5 and 4.7 wt%), the yields were far lower after cycle 3 (alkylphenolics 12.2 wt% and aromatics 3.0 wt%). Also, the total monomer yield for cycle 1 and 2 was similar (31.3 and 29.1 wt%) while this yield was decreased after cycle 3 (22.8 wt%).

Table 3.9 Monomeric product yield based on the lignin intake for the 3 reactions cycles performed using the 1%Ru-TiO_2 catalyst

1%Ru-TiO_2	Cycle 1	Cycle 2	Cycle 3
Alkylphenolics	16.1	16.2	12.2
Catecholics	2.5	2.5	0.9
Guaiacolics	1.3	2.9	0.7
Alkanes	0.3	0.3	0.5
Aromatics	4.5	4.7	3.0
Ketones	0.3	0.3	0.3
Cyclohexanes	2.9	0.8	1.6
Naphthalenes	3.4	1.4	3.6
Monomer yield %	31.3	29.1	22.8

GPC

Fig. 3.10 shows the GPC chromatogram of the lignin oil from the recycle study of the 1%Ru-TiO_2 catalyst. The deactivation of the catalyst was observed by a decrease in lignin oil yield. However, the deactivation of the catalyst did not increase the M_w of the lignin oil, since the average M_w of cycle 1,2 and 3 were respectively 200, 200 and 195 g mol^{-1}, the same effect was observed for M_w of the lignin oils obtained from the regenerated catalysts (Table 3.6). Also, the GPC chromatogram of the lignin oil from the 3 cycles does not show significant differences.

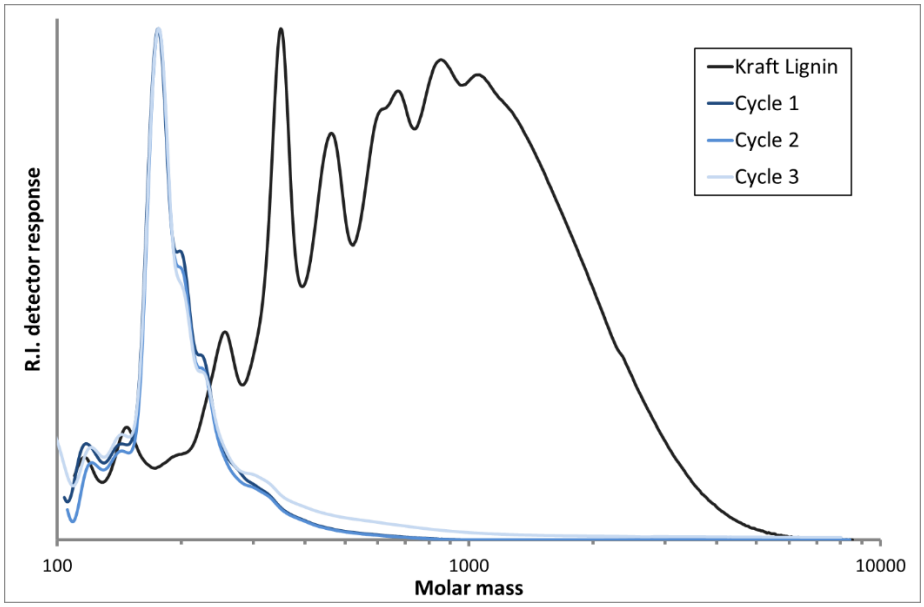

Fig. 3.10 GPC chromatogram of Kraft lignin, and cycle 1 to 3 with the 1% Ru-TiO_2 catalyst

Fresh and regenerated catalyst characterization

The fresh and regenerated catalysts were characterized using BET analysis, XRD and TEM analysis. In some cases, a sample of fresh catalyst was also subjected to regeneration conditions (designated as "freshly regenerated catalyst"), in order to be able to discriminate between the changes that take place due to hydrotreatment-regeneration combined, or just due to regeneration itself. The results are shown in the following section.

XRD

The XRD pattern of fresh, regenerated and freshly regenerated catalysts are shown in Fig. 3.11. For the case of the TiO_2 catalysts (Fig. 3.11 a and b), the majority of the peaks can be assigned to rutile TiO_2. The rutile pattern was also observed in the fresh, regenerated and freshly regenerated samples, which means the rutile structure is stable during reaction and regeneration. The characteristic peak of anatase TiO_2 (35), was observed in the fresh and freshly regenerated samples which agrees with the specifications of the TiO_2 support, this contains ~5% anatase. The anatase peak is not observed in the pattern of the regenerated catalyst, indicating that the anatase structure is not stable under hydrothermal conditions (36). Also, the structure of the 0.3%Ru-ZrO_2 catalyst (Fig. 3.11 c) was stable during reaction and regeneration conditions. All the peaks are assigned to the peaks of monoclinic ZrO_2 (37). For the case of the 1%Ru-SiO_2 catalyst (Fig. 3.11 b), the fresh and freshly regenerated catalyst showed an amorphous structure, indicated by the lack of peaks in the XRD pattern. Meanwhile the regenerated catalyst resembles the pattern of quartz with the characteristic peaks at 21.8 and 26.6 2θ (38). The hydrothermal conditions during the reaction cause the phase transformation of amorphous to quartz. This leads to a drop of surface area because Si-OH groups react during a phase transition and form water and siloxane (Si-O-Si) and consequently, the pores collapse (39). Also, the structure of the 1%Ru-Al_2O_3 catalyst (Fig. 3.11 a) was unstable during hydrotreatment conditions, due to the formation of boehmite and α-Al_2O_3. The XRD pattern of the fresh Al_2O_3 catalyst matches the pattern of γ-Al_2O_3 with peaks at 67.2 and 45.5 2θ (40). Also the pattern of freshly regenerated and regenerated catalyst resembled the γ-Al_2O_3 nevertheless, additional peaks were observed which were assigned to boehmite and α-Al_2O_3. Under hydrothermal conditions γ-Al_2O_3 is not stable and transforms to boehmite and α-Al_2O_3 (41). More peaks are observed in the pattern of regenerated Al_2O_3 than in freshly regenerated Al_2O_3. This is due to the harsh condition during

hydrotreatment with the formation of water, high temperature and pressure. The conditions during regeneration are less harsh, pressure is atmospheric and water is only available as vapor in the air.

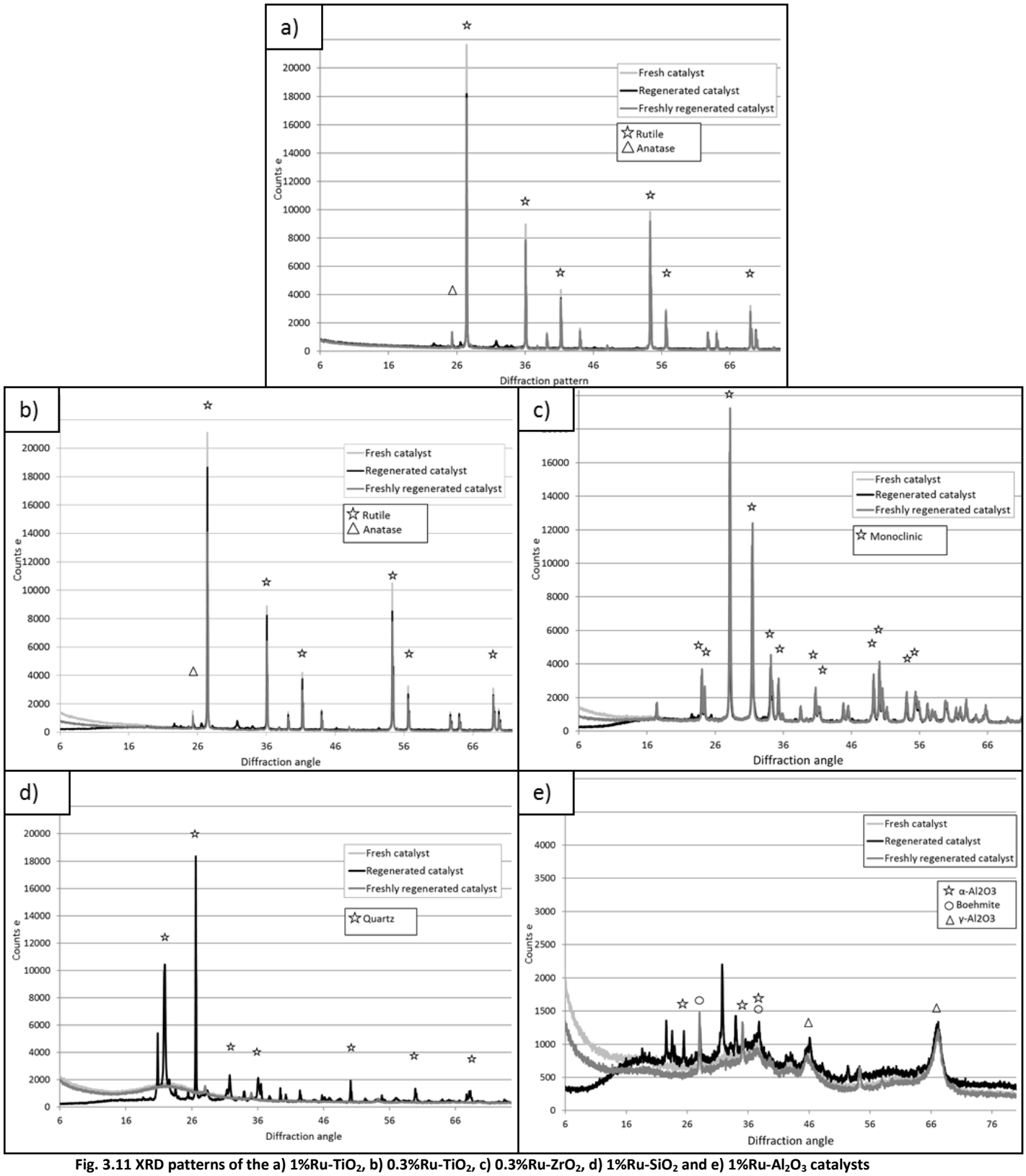

Fig. 3.11 XRD patterns of the a) 1%Ru-TiO_2, b) 0.3%Ru-TiO_2, c) 0.3%Ru-ZrO_2, d) 1%Ru-SiO_2 and e) 1%Ru-Al_2O_3 catalysts

BET surface area

BET surface area of the fresh and regenerated catalysts are presented in Table 3.10.

Table 3.10 BET surface area (m^2g^{-1}) of fresh and regenerated catalysts

Catalyst	Fresh	Regenerated
1%Ru-Al_2O_3	157.2	55.1
1%Ru-SiO_2	522.7	2.1
1%Ru-TiO_2	5.3	2.3
0.3%Ru-TiO_2	2.7	2.7
0.3%Ru-ZrO_2	5.2	3.2

The adsorption isotherms were compared to the isotherms classified by IUPAC (42). The adsorption isotherm of the fresh 1%Ru-Al_2O_3 catalyst matches the type II isotherm but also shows similarities of the type IV isotherm. Therefore, the fresh 1%Ru-Al_2O_3 catalyst has a porous structure with both meso and macro pores. The adsorption isotherm of regenerated 1%Ru-Al_2O_3 catalyst matches type II isotherm which indicates that the catalyst has a macroporous structure. The adsorption isotherm of fresh 1%Ru-SiO_2 matches the type IV adsorption isotherm which indicates a mesoporous structure. The 1%Ru and 0.3%Ru-TiO_2 and 0.3%Ru-ZrO_2 catalyst display a low BET surface area and the isotherms do not match one of the adsorption isotherm classified by IUPAC. A similar adsorption isotherm and BET surface area was seen for regenerated 1%Ru-SiO_2. (43) (42)

The low surface area of the 1%Ru and 0.3%Ru-TiO_2 and 0.3%Ru-ZrO_2 catalyst can be explained by the results of XRD. This showed a monoclinic structure for the fresh and regenerated 0.3%Ru-ZrO_2 catalyst and a rutile structure for the fresh and regenerated 1%Ru and 0.3%Ru-TiO_2 catalyst, monoclinic ZrO_2 and rutile TiO_2 are characteristic for their low surface areas (44).

After reaction and regeneration, a decrease in surface area was observed for all the catalysts, except the 0.3%Ru-TiO_2 catalyst. The most significant decrease in surface area was observed for the 1%Ru-Al_2O_3 catalyst (157.2 to 55.1 m^2g^{-1}) and for the 1%Ru-SiO_2 catalyst (522.7 to 2.1 m^2g^{-1}). The decrease of surface area for the 1%Ru-SiO_2 catalyst was caused by the phase transition observed with XRD (Fig 3.11 d).

TEM

The size and dispersion of Ru particles were analyzed with TEM pictures. To determine if metal agglomeration occurred during hydrotreatment and/or regeneration, both fresh and regenerated catalysts were analyzed. The TEM pictures of the fresh and regenerated catalysts are shown in appendix 4 and the average particle size of Ru is shown in Table 3.11. The average particle size of Ru was determined based on a particle size distribution of 10-15 particles.

Table 3.11 Average Ru particle (nm) as measured for the different fresh and regenerated catalysts

Catalyst	Fresh	Regenerated
1%Ru-Al_2O_3	4.9	10.2
1%Ru-SiO_2	2.5	15.6
1%Ru-TiO_2	2.9	7.6
0.3%Ru-TiO_2	6.5	13.5
0.3%Ru-ZrO_2	3.8	6.7

Out of all the regenerated catalysts, the 1%Ru-TiO_2 catalyst showed the highest lignin oil and monomeric products yield. The catalysts activity was explained with Ru particle dispersion, shown in Fig. 3.12 a and b. For

the fresh catalyst, highly dispersed and small particles (2.9 nm) were observed while the regenerated catalysts showed an increased particle size of 7.6 nm. However, in comparison with the other regenerated catalysts, the Ru particles remained small and clustering of particles was not significant.

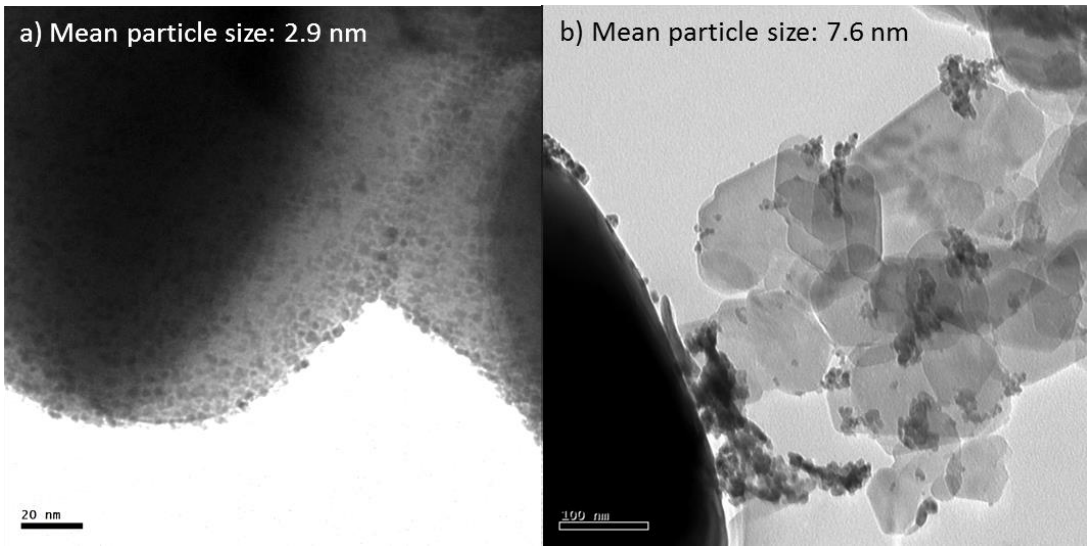

Fig. 3.12 TEM pictures of a) fresh and b) regenerated 1%Ru-TiO_2 catalyst

The 1%Ru-SiO_2 catalyst showed the most deactivation, the yields of lignin oil and monomeric products were significantly decreased after regeneration. The TEM pictures (appendix 4) showed that the Ru particle size increased from 2.5 to 15.6 nm. The particles were highly dispersed on the surface of the fresh catalyst while the surface of the regenerated catalyst showed clusters of metal particles. Also, the phase transition of SiO_2, confirmed by XRD, was observed by TEM analysis since the fresh catalyst showed an amorphous structure and the regenerated catalyst showed a more crystal, needle-like structure.

TEM analysis showed for the 1%Ru-Al_2O_3, 0.3%Ru-ZrO_2 and 0.3%Ru-TiO_2 catalysts an increase in Ru particle size after regeneration from 4.9 to 10.2, 3.8 to 6.7 and 6.5 to 13.5 nm, respectively. The least significant particle increase was observed for the 0.3%Ru-ZrO_2 catalyst. However, the particles were clustered and the majority of surface area was not covered with metal particles. Therefore, a substantial decrease in lignin oil and monomer yield was observed when the regenerated 0.3%Ru-ZrO_2 catalyst was used while the Ru particle size did not increase significantly. The increase in metal particle size of the 1%Ru-Al_2O_3 and 0.3%Ru-TiO_2 catalysts resulted in lower lignin oil and monomeric products yields when the regenerated catalysts were used.

Discussions and conclusion

Hydrotreatment of Kraft lignin was performed with different Ru-based catalysts on various supports (Al_2O_3, SiO_2, ZrO_2 and TiO_2) with different metal loadings (0.3 and 1 wt%). To be able to correlate the physico-chemical properties of the catalyst with their performance BET analysis, XRD and TEM analysis were executed.

In terms of product distributions, the difference regarding lignin oil yield (the main product fraction in all cases) using the fresh catalysts was not significant with yields between 35-40 wt%, while the solid yields were in between 17-22 wt%, water yields of 20-21 wt% and gas yields in the range of 14-16 wt%. The same observation was made for the yields of alkylphenolics and aromatics, these were in the range of 14-16 wt% and ≈4 wt%, respectively. The 1%Ru-TiO_2 catalyst showed the highest activity with a lignin oil yield of 39.6 wt% on lignin intake and yields of alkylphenolics and aromatics of 16.1 wt% and 4.5 wt% on lignin intake. When the oil and monomer yields were compared with previous studies, the catalysts were surprisingly active despite the low Ru loadings and the presence of sulfur.

Hydrotreatment of Kraft lignin with regenerated catalysts showed major differences between the different catalyst regarding lignin oil and monomeric product yields. When regenerated catalysts were used, only the 1%Ru-TiO_2 catalyst showed similar lignin oil yield compared to fresh catalyst conditions (39.6 to 36.7 wt% on lignin intake), while the other regenerated catalysts showed a significant decrease in lignin oil yields, in the range of 26-31 wt%. Also, a decrease in monomeric products was observed with yields of alkylphenolics and aromatics in the range of 10.8-14.3 wt% and 2.8-3.5 wt%, respectively. The 1%Ru-TiO_2 catalyst was the exception, since similar alkylphenolics (16.2 wt%) and aromatics (4.7 wt%) yields were obtained in comparison to when the catalyst was applied in fresh conditions. Therefore, the regenerability of the 1%Ru-TiO_2 catalyst was further explored in a recycling study with a total of 3 reaction cycles, wherein the catalyst showed a gradual deactivation.

XRD showed that the supports structure of 1%Ru-Al_2O_3 and 1%Ru-SiO_2 catalysts were not stable during hydrotreatment, since the structure of Al_2O_3 and SiO_2 evolved towards the formation of boehmite, α-Al_2O_3 and quartz, which had a significant impact on the catalysts activity. On the other hand, the 0.3% and 1% Ru-TiO_2 and 0.3%Ru-ZrO_2 catalysts were stable during hydrotreatment and the crystalline structure does not suffer significant modifications after hydrotreatment and subsequent regeneration. However, the 0.3%Ru-TiO_2 and 0.3%Ru-ZrO_2 catalysts showed a significant decrease in activity after regeneration, which can be mainly assigned to the agglomeration of Ru particles, observed by TEM analysis.

TEM analysis showed that the agglomeration of Ru particles has an important impact on lignin oil and monomer yields when regenerated catalysts were applied. The Ru particles of the 1% Ru-TiO_2 catalyst were smaller and less clustered, which correlates with the similar performance of the catalyst in fresh and regenerated conditions. Bimetallic catalysts are more stable than monometallic catalysts due to a less extent of metal agglomeration (45). Therefore, it would be interesting to study the regenerability of bimetallic catalysts for Kraft lignin hydrotreatment.

While this research focused on the regenerability of the catalysts in a batch reactor, in the future further studies in a continuous setup could be performed in order to determine the stability of the catalyst with time of reaction. Preferably, less complex and cleaner feed (like lignin model compounds) could be used, in order to be able to also analyse the catalyst after reaction without the need of a regeneration step and gather insights into the effect of both coke formation and the effect of sulfur.

Major differences were observed between the activity of the regenerated catalysts, this was not the case for the fresh catalysts. Only the 1%Ru-TiO_2 catalyst showed similar reaction results in fresh and regenerated conditions. The cause for catalyst deactivation was mainly assigned to instability of the support and/or agglomeration of Ru particles. Further studies have to determine the catalysts stability in a continuous set up.

References

1. **A. Kloekhorst, H.J. Heeres.** *PhD Thesis: Biobased Chemicals from Lignin.* Groningen : Rijksuniversiteit Groningen, 2015.

2. *Production of first and second generation biofuels: A comprehensive review.* **S.N. Naik, Vaibhav V. Goud, Prasant K. Rout, Ajay K. Dalai.** 2, sl : Renewable and Sustainable Energy Reviews, 2010, Renewable and Sustainable Energy Reviews, Vol. 14, pp. 578-597.

3. **Lin, C. W. Dence and S. Y.** *Methods in Lignin Chemistry.* sl : Springer Berlin Heidelberg, 1992.

4. *Aromatic Monomers by in Situ Conversion of Reactive Intermediates in the Acid-Catalyzed Depolymerization of Lignin.* **P. J. Deuss, M. Scott, F. Tran, N. J. Westwood, J. G. de Vries and K. Barta.** 2015 : Journal of the American Chemical Society, Vol. 137, pp. 7456–7467.

5. *Paving the Way for Lignin Valorisation: Recent Advances in Bioengineering, Biorefining and Catalysis.* **R. Rinaldi, R. Jastrzebski, M. T. Clough, J. Ralph, M. Kennema, P. C. A. Bruijnincx and B. M. Weckhuysen.** sl : Angew. Chem. Int. Ed., 2016, Vol. 55, pp. 8164-8215.

6. **Bajpai, P.** *Pretreatment of Lignocellulosic Biomass for Biofuel Production.* sl : Springer, 2016.

7. **Pinkerfon, A. V. Someshwar and J. E.** *Wood Processing Industry.* 1992.

8. *Changes for Biomass: Integrated valorisation of Biomass Resources.* Wageningen : Wageningen UR, 2012.

9. *Solvent free depolymerization of Kraft lignin to alkyl-phenolics using supported NiMo and CoMo catalysts.* **C. R. Kumar, N. Anand, A. Kloekhorst, C. Cannilla, G. Bonura, F. Frusteri, K. Barta and H. J. Heeres.** 11, sl : Green Chemistry, 2015, Green Chemistry, Vol. 17, pp. 4921-4930.

10. *The Catalytic Valorization of Lignin for the Production of Renewable Chemicals.* **J. Zakzeski, P. C. A. Bruijnincx, A. L. Jongerius and Bert M. Weckhuysen.** 6, sl : Chemical Reviews, 2010, Vol. 110, pp. 3552-3599.

11. *Discovery and Characterization of Heme Enzymes from Unsequenced Bacteria: Application to Microbial Lignin Degradation.* **M. E. Brown, M. C. Walker, T. G. Nakashige, A. T. Iavarone and M. C. Y. Chang.** 45, sl : Journal of American Chemical Society, 2011, Vol. 133, pp. 18006-18009.

12. *Towards Quantitative Catalytic Lignin Depolymerization.* **V. M. Roberts, V. Stein, T. Reiner, A. Lemonidou, X. Li and J. A. Lercher.** 21, sl : Chemistry a European Journal, 2011, Vol. 17, pp. 5939-5948.

13. *Formic-acid-induced depolymerization of oxidized lignin to aromatics.* **A. Rahimi, A. Ulbrich, J. J. Coon and S. S. Stahl.** sl : Nature, 2014, Vol. 515, pp. 249-252.

14. *Heterogeneously catalyzed lignin depolymerization.* **Lee, A. Pineda and A.F.** sl : Appl Petrochem Res, 2016, Vol. 6.

15. *Trends in analytical methodologies for the determination of alkylphenols and bisphenol A in water samples.* **N. Salgueiro-Gonzalez, S. Muniategui-Lorenzo, P. Lopez-Mahía, D. Prada-Rodríguez.** sl : Analytica Chimica Acta, 2017, Vol. 962, pp. 1-14.

16. *Mechanisms of Membrane Toxicity of Hydrocarbons.* **J. Sikkema, J.A.M. de Bont, B. Poolman.** 2, sl : Microbiological Reviews, 1995, Vol. 59, pp. 201-222.

17. *Sustainable bisphenols from renewable softwood lignin feedstock for polycarbonates and cyanate ester resins.* **S.F. Koelewijn, S. Van den Bosch, T. Renders, W. Schutyser, B. Lagrain, M. Smet, J. Thomas, W. Dehaen, P. Van Puyvelde, H. Witterse and B. F. Sels.** 11, sl : Green Chemistry, 2017, Vol. 19, pp. 2561-2570.

18. *Replacing bisphenol-A with bisguaiacol-F to synthesize polybenzoxazines for a pollution-free environment.* **T. Periyasamy, S. P. Asrafali, S. Muthusamy and S-C. Kim.** 11, sl : New Journal of Chemistry, 2016, Vol. 40, pp. 9313–9319.

19. *Selective Conversion of Lignin-Derivable 4-Alkylguaiacols to 4-Alkylcyclohexanols over Noble and Non-Noble-Metal Catalysts.* **W. Schutyser, G. vd. Bossche, A. Raaffels, S. vd. Bosch, S-F. Koelewijn, T. Renders, and B. F. Sels.** 10, sl : ACS Sustainable Chemistry & Engineering, 2016, Vol. 4, pp. 5336-5346.

20. *Reductive Depolymerization of Kraft and Organosolv Lignin in Supercritical Acetone for Chemicals and Materials.* **Z. Yuan, M. Tymchyshyn, C. Xu.** 11, sl : ChemCatChem, 2016, Vol. 8, pp. 1968-1976.

21. *Lignin Valorisation for Chemicals and (Transportation) Fuels via (Catalytic) Pyrolysis and Hydrodeoxygenation.* **P. de Wild, R. Van der Laan, A. Kloekhorst and E. Heeres.** 3, sl : Environmental Progress & Sustainable Energy, 2009, Vol. 28, pp. 461–469.

22. *Depolymerization of lignin via a non-precious Ni–Fe alloy catalyst supported on activated carbon.* **Y. Zhai, C. Li, G. Xu, Y. Ma, X. Liu and Y. Zhang.** sl : Green Chemistry, 2017, Vol. 19, pp. 1895-1903.

23. *Catalytic ethanolysis of Kraft lignin into high-value small-molecular chemicals over a nanostructured α-molybdenum carbide catalyst.* **R. Ma, W. Hao, X. Ma, Y. Tian, Y. Li.** 28, sl : Angewandte Chemie International Edition, 2014, Vol. 53, pp. 7310-7315.

24. *Experimental Studies on the Hydrotreatment of Kraft Lignin to Aromatics and Alkylphenolics Using Economically Viable Fe-Based Catalysts.* **S. Agarwal, R. K. Chowdari, I. Hita and H. J. Heeres.** 3, sl : ACS Sustainable Chemistry & Engineering, 2017, Vol. 5, pp. 2668-2678.

25. *Mechanisms of catalyst deactivation.* **Bartholomew, C. H.** sl : Applied Catalysis A: General, 2001, Vol. 212, pp. 17-60.

26. *Effect of Sulfur on Catalytic Gasification of Lignin in Supercritical Water.* **M. Osada, N. Hiyoshi, O. Sato, K. Arai and M. Shirai.** 3, sl : Energy Fuels, 2007, Vol. 21, pp. 1400-1405.

27. *Heterogeneous Catalytic Transfer Hydrogenation as an Effective Pathway in Biomass Upgrading.* **Xu, M.J. Gilkey and B.** 3, sl : ACS Catalysis, 2016, Vol. 6, pp. 1420-1436.

28. *Mechanistic Insights into Metal Lewis Acid-Mediated Catalytic Transfer Hydrogenation of Furfural to 2-Methylfuran.* **M. J. Gilkey, P. Panagiotopoulou, A. V. Mironenko, G. R. Jenness, D. G. Vlachos and B. Xu.** 7, sl : ACS Catalysis, 2015, Vol. 5, pp. 3988-3994.

29. *Tuning Ni nanoparticles and the acid sites of silica-alumina for liquefaction and hydrodeoxygenation of lignin to cyclic alkanes.* **J. Kong, B. Li and C. Zhao.** 76, sl : RSC Advances, 2016, Vol. 6, pp. 71940-71951.

30. *Sorbitol hydrogenolysis to glycols by supported ruthenium catalysts.* **I. M. Leo, M. L. Granados, J. L. G. Fierro and R. Mariscal.** 5, sl : Chinese Journal of Catalysis, 2014, Vol. 35, pp. 614-621.

31. *Catalyst studies on the hydrotreatment of fast pyrolysis oil.* **J. Wildschut, I. Melián-Cabrera and H.J. Heeres.** 1, sl : Applied Catalysis B: Environmental, 2010, Vol. 99, pp. 298-306.

32. **Farrauto, C. H. Bartholomew and R. J.** *Fundamentals of Industrial Catalytic Processes, Second Edition.* sl : John Wiley & Sons, 2006.

33. *Influence of the support on sulfur poisoning and regeneration of Ru catalysts probed by sulfur K-edge X-ray absorption spectroscopy.* **C. König, F. J. Schuh, P. Huthwelker, T. Smolentsev, G. Schildhauer, J. Tilman and M. Nachtegaal.** sl : Catalysis Today, 2014, Vol. 229, pp. 56-63.

34. *Heterogeneous Catalyst Deactivation and Regeneration: A Review.* **Bartholomew, M. D. Argyle and C. H.** 1, sl : Catalysts, 2015, Vol. 5, pp. 145-269.

35. *Effect of brookite phase on the anatase–rutile transition in titania nanoparticles.* **Y. Hu, H.- L. Tsai, C.- L. Huang.** 5, sl : Journal of the European Ceramic Society, 2003, Vol. 23, pp. 691-696.

36. *Effect of support synthesis methods on structure and performance of VOx/CeO2 catalysts in low-temperature NH3-SCR of NO.* **T.H. Vuong, J. Radnik, M. Schneider, H. Atia, U. Armbruster and A Brückner.** sl : Catalysis Communications, 2016, Vol. 84, pp. 171-174.

37. *Effects of Hydrothermal Conditions of ZrO2 on Catalyst Properties and Catalytic Performances of Ni/ZrO2 in the Partial Oxidation of Methane.* **Y. Song, H. Liu and D. He.** 5, sl : Energy Fuels, 2010, Vol. 24, pp. 2817-2824.

38. *A high-pressure synthesis of hydrothermally stable periodic mesoporous crystalline aluminosilica materials.* **M. Mandal, A. S. Manchanda, C. Liu, Y. Fei and K. Landskron.** 9, sl : RSC advances, 2016, Vol. 6, pp. 7396-7402.

39. **Somasundaran, P.** *Encyclopedia of Surface and Colloid Science, Second Edition.* sl : CRC Press, 2006.

40. *Effect of mill type on the size reduction and phase transformation of gamma alumina.* **S.R. Chauruka, A. Hassanpour, R. Brydson, K.J. Roberts, M. Ghadiri and H. Stitt.** sl : Chemical Engineering Science, 2015, Vol. 134, pp. 774-783.

41. *Preparation of Nanocrystalline Alumina under Hydrothermal Conditions.* **O. V. Al'myasheva, E. N. Korytkova, A. V. Maslov and V. V. Gusarov.** 5, sl : Inorganic Materials, 2005, Vol. 41, pp. 460-467.

42. *Surface area and pore texture of catalysts.* **G. Leofanti, M. Padovan, G. Tozzola, B. Venturelli.** 1, sl : Catalysis Today, 1998, Vol. 41, pp. 207-219.

43. *The use of nitrogen adsorption for the characterisation of porous materials.* **Sing, K.** sl : Colloids and Surfaces A: Physicochemical and Engineering Aspects, 2001, Vol. 187, pp. 3-9.

44. **Busca, G.** Metal Oxides as Acid-Base Catalytic Materials. *Heterogeneous Catalytic Materials.* sl : Elsevier, 2014.

45. *Stability of Bimetallic Reforming Catalysts.* **Beltramini, J. M. Parera AND J. N.** 2, sl : Journal of Catalysis, 1988, Vol. 112, pp. 357-365.

Appendix

1. Material details

	Purity	Supplier	Product specification
Ru-(acac)3	97%	Sigma Aldrich (SA)	282766-59
Kraft lignin		Meadwestvaco Specialty Chemical	
Alumina (γ-alumina)		SA	05184-100G
Silica (amorphous)		Silicycle	R090817003
Zirconia (monoclinic)	99%	SA	230693-100G
Titania (rutile with ~5% anatase)	99%	SA	224227-100G
Acetone	>95%	Boom	76050006
DCM		Boom	76045212
Methanol	99.8%	SA	322415-1L
Acetonephenone	99%	SA	00790-250ml
THF		Boom	76625397-2500
DBE	99.5%	SA	175943-50G
Toluene	99.5%	Lab-scan	
DMSO	99.3%	SA	271454-100ml
Hydranal		Riedel de Haen	34698-1L
Karl Fischer Composit 5K		Riedel de Haen	34816-1L
Nitrogen		Linde	UN1066
Hydrogen		Linde	UM1049
CO_2		Linde	UN1013
Refgas		Westfalen	UN1953

2. Elemental analysis

Catalysts	**Weight**		**Atomic ratio**	
	H/C	O/C	H/C	O/C
Kraft Lignin	0,096	0,477	1,151	0,358
Fresh	H/C	O/C	H/C	O/C
1%Ru-Al_2O_3	0,089	0,088	1,071	0,066
1%Ru-SiO_2	0,090	0,094	1,079	0,070
1%Ru-TiO_2	0,090	0,093	1,079	0,070
0,3%Ru-TiO_2	0,088	0,096	1,059	0,072
0,3%Ru-ZrO_2	0,090	0,092	1,085	0,069
Regenerated	H/C	O/C	H/C	O/C
1%Ru-Al_2O_3	0,091	0,103	1,089	0,077
1%Ru-SiO_2	0,102	0,260	1,227	0,195
1%Ru-TiO_2	0,091	0,128	1,095	0,096
0,3%Ru-TiO_2	0,093	0,162	1,118	0,121
0,3%Ru-ZrO_2	0,094	0,125	1,130	0,094
Cycle 3	H/C	O/C	H/C	O/C
1%Ru-TiO_2	0,088	0,121	1,057	0,090

3. Relative concentrations of monomeric products

	1% Ru-Al2O3		1% Ru-SiO2		0.3%Ru-Zr02	
	fresh	reg	fresh	reg	fresh	reg
AlkylPhenolics	40.3	46.7	39.1	39.3	39.5	50.5
Catecholics	4.5	4.6	6.5	3.7	5.9	6.6
Guaiacolics	1.9	1.2	2.4	0.9	2.8	2.4
Alkanes	0.9	2.5	1.3	0.3	1.0	0.6
Aromatics	11.9	10.4	9.9	10.3	10.0	13.2
Ketones	0.8	1.4	0.8	1.6	0.8	2.4
Cyclohexanes	8.3	5.8	7.5	6.7	7.5	4.7
Naphthalenes	8.9	7.6	8.1	6.0	8.8	9.8

	0.3% Ru-TiO2		1% Ru-TiO2		
	fresh	reg	fresh	reg	cycle 3
AlkylPhenolics	40.3	46.8	40.5	44.2	39.2
Catecholics	4.4	5.3	6.2	6.8	3.0
Guaiacolics	2.8	1.2	3.3	8.0	2.2
Alkanes	1.1	0.6	0.9	0.8	1.7
Aromatics	9.7	10.9	11.4	12.9	9.6
Ketones	0.8	2.0	0.6	0.9	1.1
Cyclohexanes	6.6	4.8	7.2	2.3	5.1
Naphthalenes	8.3	7.2	8.5	3.7	11.5

4. TEM pictures

Fresh 1%Ru-SiO_2
mean particle size: 2.5 nm

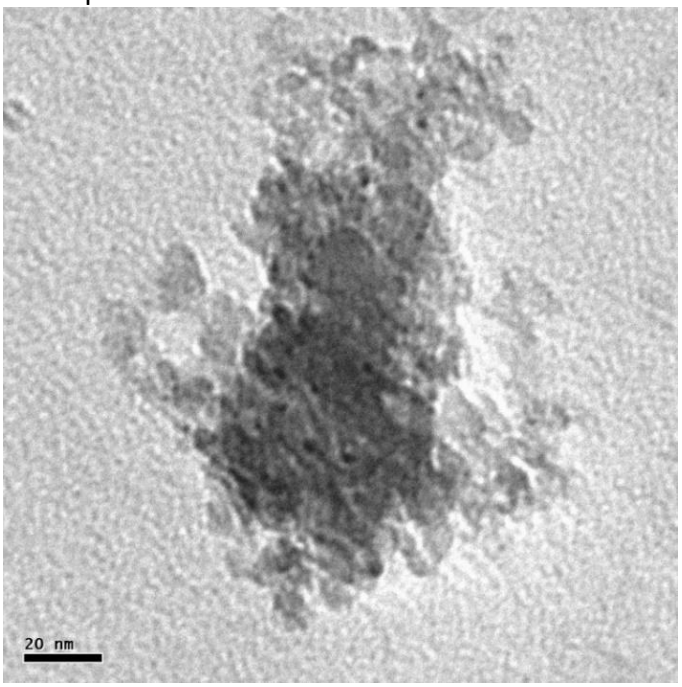

Regenerated 1%Ru-SiO_2
mean particle size: 15.6 nm

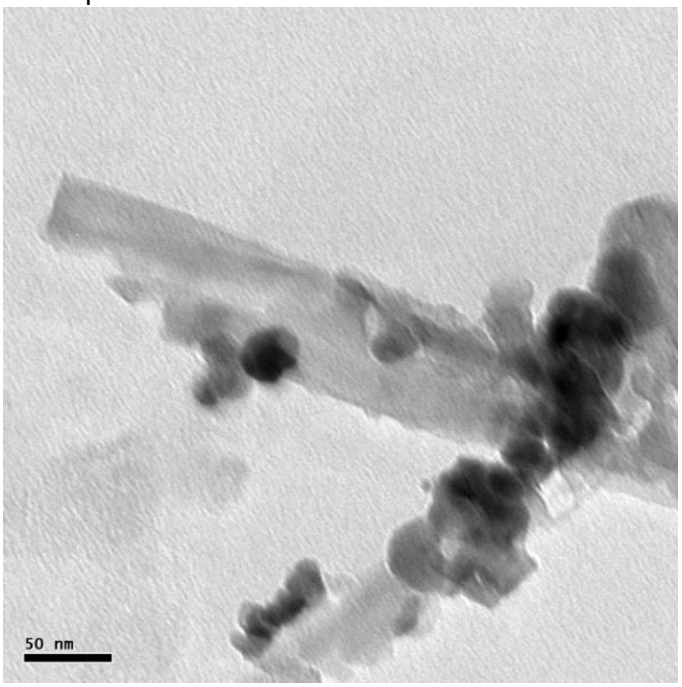

Fresh 0.3%Ru-TiO_2
mean particle size: 6.5 nm

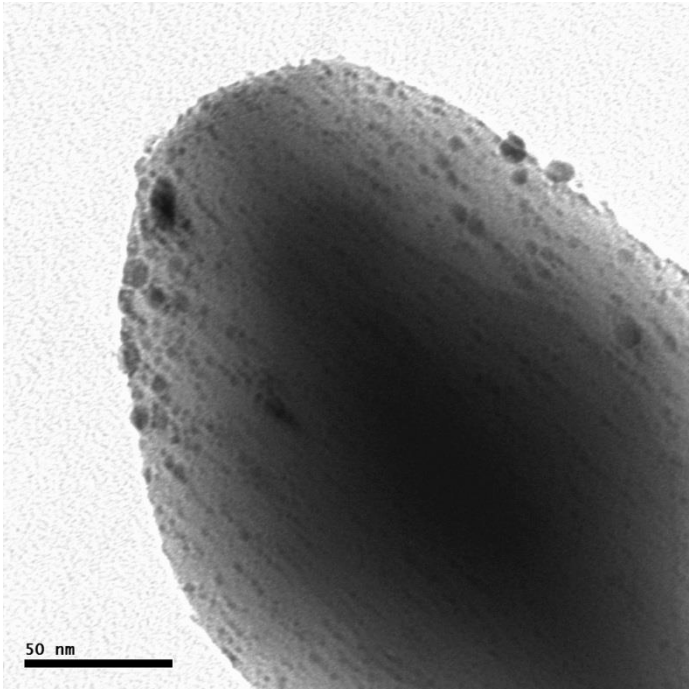

Regenerated 0.3%Ru-TiO_2
mean particle size: 13.5 nm

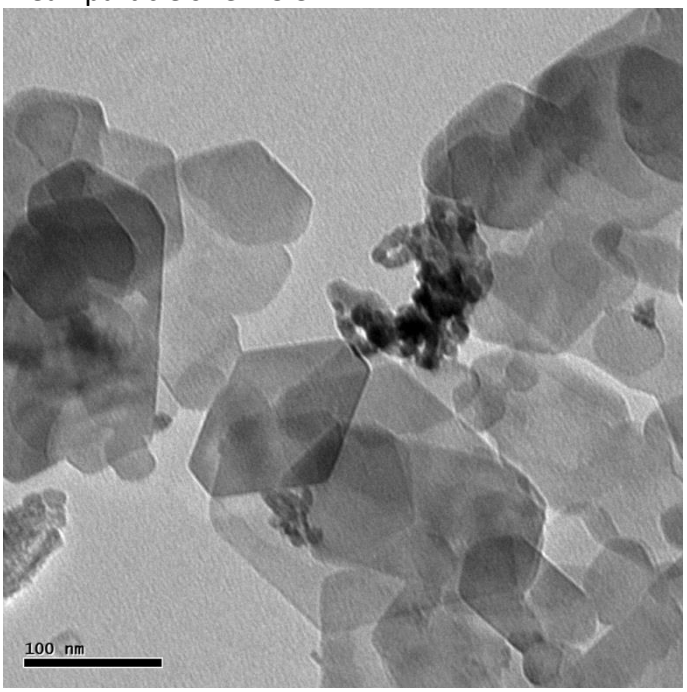

Fresh 1%Ru-TiO_2
mean particle size: 2.9 nm

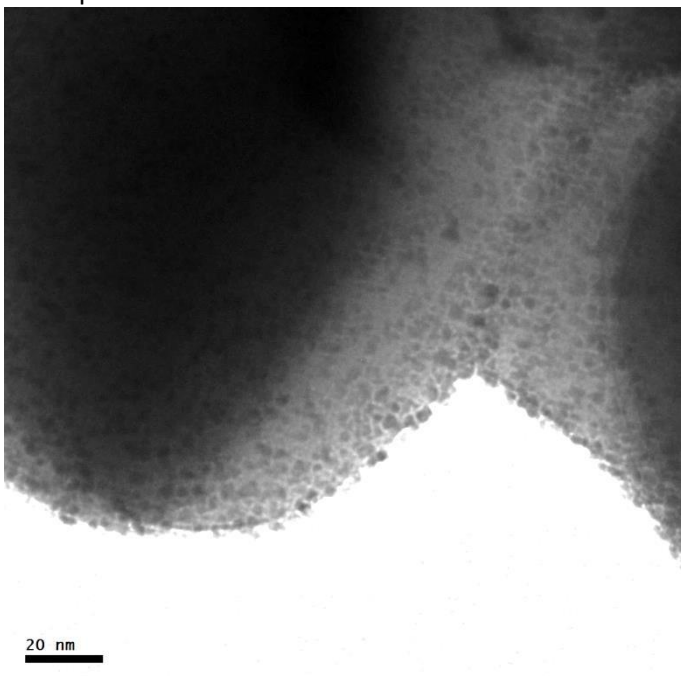

Regenerated 1%Ru-TiO_2
mean particle size: 7.6 nm

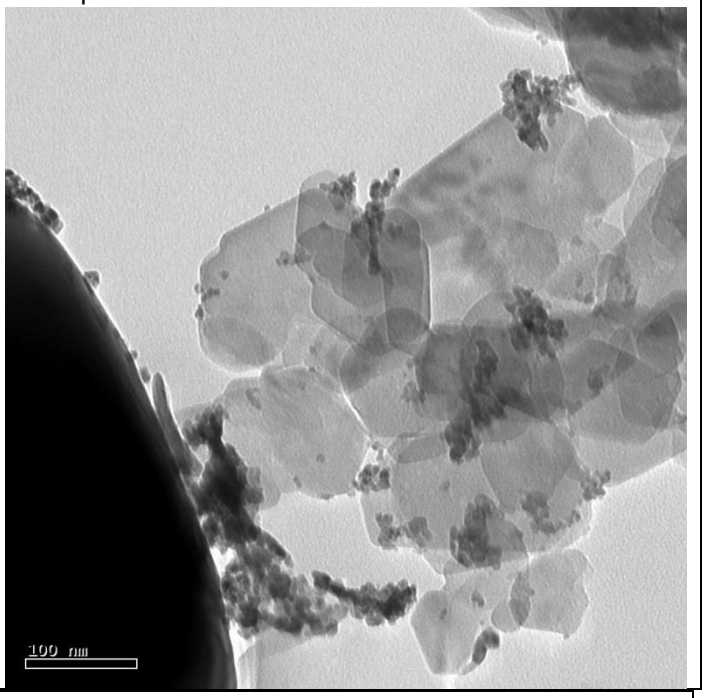

Fresh 0.3%Ru-ZrO_2
mean particle size: 3.8 nm

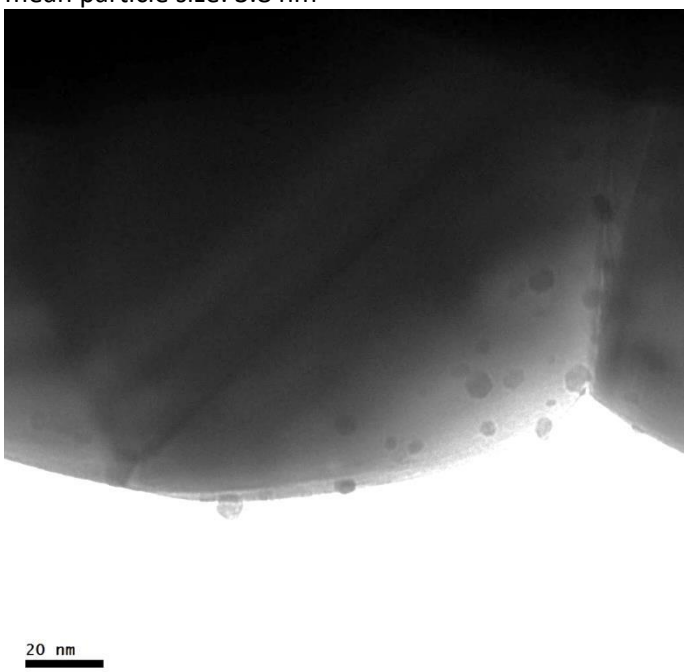

Regenerated 0.3%Ru-ZrO_2
mean particle size: 6.7 nm

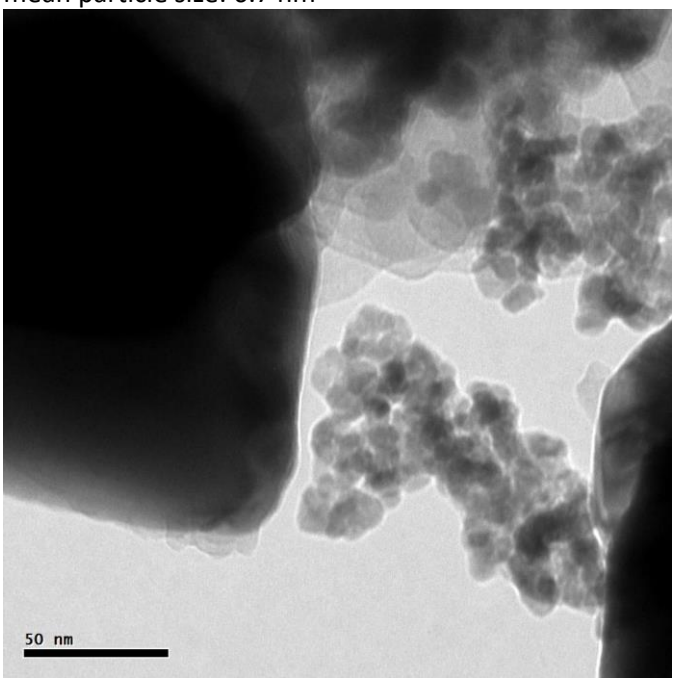

Fresh 1%Ru-Al_2O_3 mean particle size: 4.9 nm	Regenerated 1%Ru- Al_2O_3 mean particle size: 10.2 nm
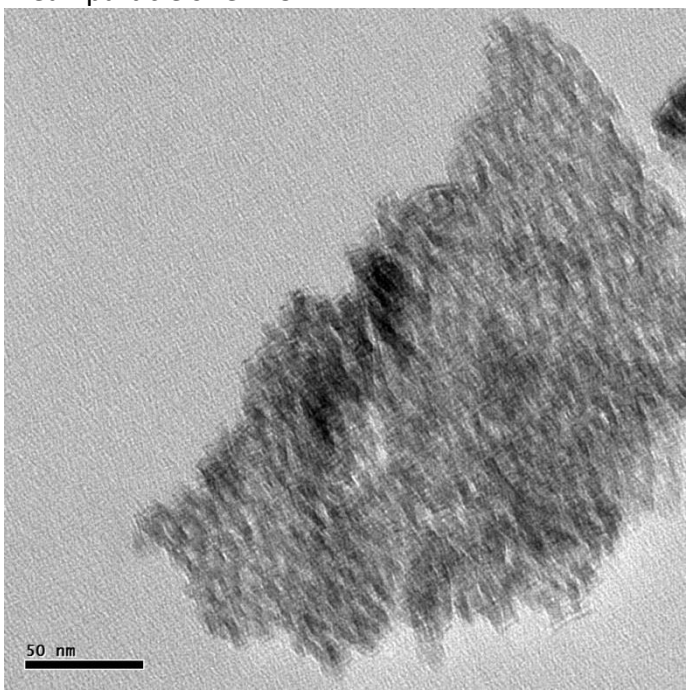	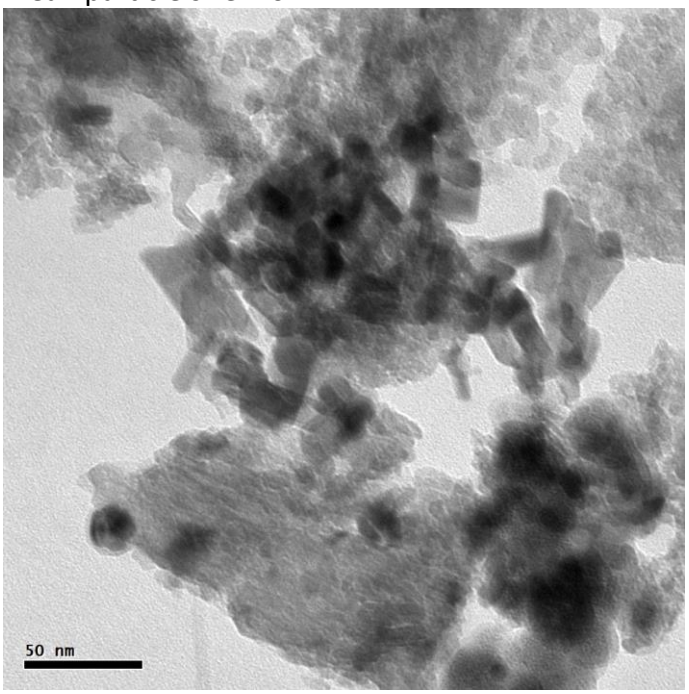

5. Reaction with solids

From the reactions with regenerated catalyst, solids were obtained which contained an excessive amount of coke. The activity of the catalyst, covered in coke, was explored in a reaction with Kraft lignin and solids obtained from the reaction with the 0.3%Ru-ZrO_2 regenerated catalysts. The reaction yielded a black solid material (showed on the picture) and no oil or water phase was observed. The lack of oil phase indicates that regeneration is crucial to remain catalytic activity.